

# 1 Extinct Radionuclides and the Earliest Differentiation of the Earth and Moon

G. CARO<sup>1</sup> AND T. KLEINE<sup>2</sup>

<sup>1</sup>CRPG-CNRS, Nancy Université, Vandoeuvre-les-Nancy, France

<sup>2</sup>Institut für Planetologie, Westfälische Wilhelms-Universität Münster, Münster, Germany

## SUMMARY

The extinct  $^{182}\text{Hf}$ - $^{182}\text{W}$  and  $^{146}\text{Sm}$ - $^{142}\text{Nd}$  systems provide key chronological constraints on the major episodes of planetary differentiation. Both chronometers can be considered extinct after approximately 5–6 half-lives (i.e., after 50 Myr and 400 Myr respectively) and are therefore selectively sensitive to early events. Application of  $^{182}\text{Hf}$ - $^{182}\text{W}$  chronometry shows that segregation of the Earth's core may have been complete no earlier than 30 Myr after formation of the solar system and probably involved at least partial re-equilibration of newly accreted metallic cores within the terrestrial magma ocean. The current best estimate for the termination of the major stage of Earth's accretion and segregation of its core is provided by the age of the Moon, which formed as a result of a giant collision of a Mars-sized embryo with the proto-Earth. According to  $^{182}\text{Hf}$ - $^{182}\text{W}$  systematics this event occurred 50–150 Myr after CAI formation. As the Earth cooled down following the giant impact, crystallization of the magma ocean resulted in the formation of the earliest terrestrial crust. While virtually no remnant of this proto-crust sur-

vived in the present-day rock record, the isotopic fingerprint of this early event is recorded in the form of small  $^{142}\text{Nd}$  anomalies in early Archean rocks. These anomalies show that magma ocean solidification must have taken place 30–100 Myr after formation of the solar system. In contrast,  $^{146}\text{Sm}$ - $^{142}\text{Nd}$  systematics of lunar samples show that the lunar mantle may have remained partially molten until 300 Myr after CAI formation. Therefore, extinct chronometers indicate that accretion and differentiation of the Earth proceeded rapidly. The core, mantle and crust were completely differentiated less than 100 Myr after formation of the solar system.

## INTRODUCTION

The accretion and earliest history of the Earth was an episode of major differentiation of a magnitude that probably will never be repeated. Frequent and highly energetic impacts during the Earth's growth caused widespread melting, permitting separation of a metallic core from a silicate mantle in a magma ocean. Soon after the major stages of the Earth's growth were complete, the magma ocean solidified and a first proto-crust formed. Earth is an active planet, however, concealing most of the evidence of its earliest evolutionary history by frequent rejuvenation of its crust. Consequently,

---

*Timescales of Magmatic Processes: From Core to Atmosphere*, 1st edition. Edited by Anthony Dosseto, Simon P. Turner and James A. Van Orman.  
© 2011 by Blackwell Publishing Ltd.

there is no direct rock record of the Earth's origin and earliest evolution, but fortunately witnesses of the Earth's earliest evolution have been preserved as small isotope anomalies in the terrestrial rock record. The short-lived  $^{182}\text{Hf}$ ,  $^{182}\text{W}$  and  $^{146}\text{Sm}$ - $^{142}\text{Nd}$  isotope systems provide key constraints for understanding the Earth's accretion and earliest differentiation, and in this chapter, the basic theory of these isotope systems and their application to models of the Earth's formation and differentiation will be discussed.

The starting place for the accretion of the Earth is the solar nebula, a flattened disk of gas and dust orbiting the young Sun. Within the inner regions of the solar nebula, dust grains collided and stuck together to form a large population of meter- to kilometer-sized objects. Gravity and gas drag caused these planetesimals to collide and form increasingly larger bodies in a period of runaway growth, the products of which include numerous Moon- to Mars-sized planetary embryos. Collisions among these bodies mark the late stages of accretion, culminating in the formation of a few terrestrial planets that sweep up all the other bodies. The Moon probably formed during this period and involved a 'giant impact' of a Mars-sized body with Earth at the very end of Earth's accretion (Chambers, 2004).

Planetary accretion is intimately linked with heating and subsequent melting of the planetary interiors. The decay of short-lived radioactive isotopes, especially  $^{26}\text{Al}$  ( $t_{1/2} = 0.73\text{ Myr}$ ), and collisions among the planetary embryos, caused the planetary interiors to heat up. At some critical size, melting will have started within the planetary bodies, causing separation and segregation of a metallic core (Stevenson, 1990; Rubie *et al.*, 2007). As a consequence, all major bodies of the inner solar system and also many smaller bodies, are chemically differentiated into a metallic core and a silicate mantle. However, some planetary bodies, the chondrite parent bodies, escaped differentiation. They are too small for impact heating to be significant and formed after most  $^{26}\text{Al}$

had decayed away. Chondrites thus provide information on what planetary bodies looked like before differentiation began. As such, the chondrites are invaluable archives for investigating planetary differentiation.

Melting in the interior of a planetary object permits the denser components to migrate towards the center, thereby forming a core. Metallic iron melts at lower temperatures than silicates, such that core formation can occur either by migration of molten metal through solid silicate matrix or by separation of metal droplets from molten silicate. The latter process is probably appropriate for core formation in the Earth, where giant impacts caused the formation of widespread magma oceans. Once differentiation began, it proceeded rapidly. The downward motion of dense metal melts result in the release of potential energy and hence further heating, which further triggers differentiation (Stevenson, 1990; Rubie *et al.*, 2007).

As the Earth's mantle cooled following the last giant impact, the terrestrial magma ocean started to crystallize, ultimately resulting in the formation of the earliest terrestrial crust by migration and crystallization of residual melts near the surface. This process probably took place over timescales of the order of 10,000 to 100,000 years, depending on the blanketing effect of the early atmosphere (Abe, 1997; Solomatov, 2000). As demonstrated by the presence of detrital zircon in an Archean sedimentary formation from Western Australia (Wilde *et al.*, 2001), the earliest terrestrial crust must have solidified <150 Myr after formation of the solar system. Little is known, however, about this ancient proto-crust, as subsequent mantle-crust exchanges led to a complete rejuvenation of the Earth's surface, leaving virtually no remnant older than 3.8 Gyr. Clues on the age, lifetime and composition of the Earth's crust can thus only be obtained through the study of early Archean rocks, which sampled the mantle at a time when chemical and isotopic fingerprints of the earliest differentiation processes had not been completely erased by mantle mixing.

This chapter will be divided into three sections. The first section will introduce the main concepts and the reference parameters used for constraining the chronology of core-mantle and mantle-crust differentiation using the  $^{182}\text{Hf}$ - $^{182}\text{W}$  and  $^{146}\text{Sm}$ - $^{142}\text{Nd}$  chronometers, respectively. The second section will be dedicated to the  $^{182}\text{Hf}$ - $^{182}\text{W}$  chronology of the Earth's accretion and core formation on the Earth and the Moon. The last section will examine the chronology and mechanisms of mantle-crust differentiation on the Earth, Mars and the Moon, as obtained from application of the  $^{146}\text{Sm}$ - $^{142}\text{Nd}$  system to meteorites and planetary material.

## SYSTEMATICS AND REFERENCE PARAMETERS FOR SHORT-LIVED RADIONUCLIDES

### The two-stage model for short-lived nuclide systems: $^{182}\text{Hf}$ - $^{182}\text{W}$

Tungsten has five stable isotopes, all non-radiogenic with the exception of  $^{182}\text{W}$ , which was produced by  $\beta$ -decay of the short-lived isotope  $^{182}\text{Hf}$  ( $t_{1/2} = 9$  Myr). Because W is a moderately siderophile (iron-loving) element, whilst Hf is lithophile (rock-loving), the Hf/W ratio is fractionated by processes involving segregation of metal from silicates during formation of planetary cores. The  $^{182}\text{Hf}$ - $^{182}\text{W}$  system has thus been extensively studied in order to derive chronological constraints on terrestrial accretion and core formation. The development of the Hf-W system as a chronometer of core formation goes back to the pioneering work of Lee & Halliday (1995) and Harper & Jacobsen (1996).

The siderophile behavior of W depends on several parameters including pressure, temperature and in particular oxygen fugacity. As a consequence, partitioning of W in planetary cores varies drastically among the terrestrial planets. The Hf/W ratio of the bulk silicate Earth is estimated to be  $\sim 17$ , which is significantly higher than the chondritic Hf/W ratio of  $\sim 1$ . As Hf and W are

both refractory elements, this difference cannot be accounted for by cosmochemical fractionation in the solar nebula and is thus attributed to W partitioning into the core. Hence, assuming that core formation occurred at a time when  $^{182}\text{Hf}$  was still extant, the bulk silicate Earth should have evolved towards a W isotopic composition that is more radiogenic in  $^{182}\text{W}$  compared to chondrites.

The two-stage model represents the simplest conceptual framework for calculating ages of differentiation using radiogenic systems. The formalism described below applies to core-mantle segregation but a similar development can be used for mantle-crust differentiation using the  $^{146}\text{Sm}$ - $^{142}\text{Nd}$  chronometer. In this simple model, an undifferentiated primitive reservoir experiences instantaneous differentiation at time  $t_d$ . The core and mantle reservoirs are characterized by Hf/W ratios lower and higher than the bulk Earth value, respectively, and subsequently evolve as closed systems during the second stage. The basic decay equation for the short-lived  $^{182}\text{Hf}$ - $^{182}\text{W}$  chronometer can then be obtained from the following mass balance relationship:

$$^{182}\text{Hf}(t_0) + ^{182}\text{W}(t_0) = ^{182}\text{Hf}(t) + ^{182}\text{W}(t) \quad (1)$$

where  $t_0$  is the origin of the solar system and  $t$  is time running forward from  $t_0 = 0$  to present day ( $t_p = 4.567$  Gyr). Dividing both sides of Equation (1) using a stable and non-radiogenic isotope of the daughter element (e.g.  $^{184}\text{W}$ ), we obtain, for the bulk Earth (BE):

$$\left(\frac{^{182}\text{W}}{^{184}\text{W}}\right)_{t}^{\text{BE}} = \left(\frac{^{182}\text{W}}{^{184}\text{W}}\right)_{t_0} + \left(\frac{^{182}\text{Hf}}{^{184}\text{W}}\right)_{t_0}^{\text{BE}} - \left(\frac{^{182}\text{Hf}}{^{184}\text{W}}\right)_{t_0}^{\text{BE}} \quad (2)$$

where  $(^{182}\text{W}/^{184}\text{W})_{t_0}$  is the initial W isotopic composition of the solar system.

Radioactive decay for  $^{182}\text{Hf}$  can be expressed as a function of time:

$$\left(\frac{^{182}\text{Hf}}{^{184}\text{W}}\right)_{t}^{\text{BE}} = \left(\frac{^{182}\text{Hf}}{^{184}\text{W}}\right)_{t_0}^{\text{BE}} e^{-\lambda_{182}t} \quad (3)$$

where  $\lambda_{182}$  is the decay constant of  $^{182}\text{Hf}$  of  $0.079\text{Myr}^{-1}$ . The second term on the right-hand side of Equation (2) can then be written as:

$$\left(\frac{^{182}\text{Hf}}{^{184}\text{W}}\right)_{t_0}^{BE} = \left(\frac{^{182}\text{Hf}}{^{180}\text{Hf}}\right)_{t_0} \left(\frac{^{180}\text{Hf}}{^{184}\text{W}}\right)_{t_0}^{BE} \quad (4)$$

where  $(^{182}\text{Hf}/^{180}\text{Hf})_{t_0}$  represents the initial abundance of the short-lived radionuclide at the time of formation of the solar system. The decay equation for the bulk Earth finally reads:

$$\left(\frac{^{182}\text{W}}{^{184}\text{W}}\right)_t^{BE} = \left(\frac{^{182}\text{W}}{^{184}\text{W}}\right)_{t_0} + \left(\frac{^{182}\text{Hf}}{^{180}\text{Hf}}\right)_{t_0} \left(\frac{^{180}\text{Hf}}{^{184}\text{W}}\right)_{t_0}^{BE} \times [1 - e^{-\lambda_{182}t}] \quad (5)$$

Isotopic heterogeneities due to radioactive decay are usually normalized to the composition of the bulk silicate Earth and expressed as deviations in parts per  $10^4$  using the epsilon notation:

$$\epsilon^{182}\text{W} = \left( \frac{\left(\frac{^{182}\text{W}}{^{184}\text{W}}\right)_R}{\left(\frac{^{182}\text{W}}{^{184}\text{W}}\right)_{BSE}} - 1 \right) \times 10^4 \quad (6)$$

Using this notation, the present-day chondritic  $\epsilon^{182}\text{W}$  is  $-1.9$   $\epsilon$ -units, whilst the bulk silicate Earth (BSE), by definition, has  $\epsilon^{182}\text{W} = 0$ .

In the two-stage model, differentiation occurs as an instantaneous event at  $t_d > t_0$ . The core incorporates no Hf, so that its isotopic composition during the second stage remains constant and identical to that of the bulk Earth at time  $t_d$ :

$$\left(\frac{^{182}\text{W}}{^{184}\text{W}}\right)_t^{Core} = \left(\frac{^{182}\text{W}}{^{184}\text{W}}\right)_{t_d}^{BE} = \left(\frac{^{182}\text{W}}{^{184}\text{W}}\right)_{t_0} + \left(\frac{^{182}\text{Hf}}{^{180}\text{Hf}}\right)_{t_0} \left(\frac{^{180}\text{Hf}}{^{184}\text{W}}\right)_{t_0}^{BE} \times [1 - e^{-\lambda_{182}t_d}] \quad (7)$$

The residual silicate reservoir (i.e. the bulk silicate Earth) is depleted in W and its isotopic composition evolves towards a more radiogenic  $^{182}\text{W}/^{184}\text{W}$  signature according to the following equation:

$$\left(\frac{^{182}\text{W}}{^{184}\text{W}}\right)_t^{BSE} = \left(\frac{^{182}\text{W}}{^{184}\text{W}}\right)_{t_d}^{BE} + \left(\frac{^{182}\text{Hf}}{^{180}\text{Hf}}\right)_{t_0} \left(\frac{^{180}\text{Hf}}{^{184}\text{W}}\right)_{t_0}^{BSE} \times [e^{-\lambda_{182}t_d} - e^{-\lambda_{182}t}] \quad (8)$$

Combining Equations (7) and (8), we obtain the final two-stage model equation for short-lived radionuclides:

$$\left(\frac{^{182}\text{W}}{^{184}\text{W}}\right)_t^{BSE} = \left(\frac{^{182}\text{W}}{^{184}\text{W}}\right)_{t_0} + \left(\frac{^{182}\text{Hf}}{^{180}\text{Hf}}\right)_{t_0} \left\{ \left(\frac{^{180}\text{Hf}}{^{184}\text{W}}\right)_{t_0}^{BE} \times [1 - e^{-\lambda_{182}t_d}] + \left(\frac{^{180}\text{Hf}}{^{184}\text{W}}\right)_{t_0}^{BSE} \times [e^{-\lambda_{182}t_d} - e^{-\lambda_{182}t}] \right\} \quad (9)$$

A model age for core formation can thus be directly derived from the present-day W isotopic composition and Hf/W ratio of the BSE (i.e.  $(^{182}\text{W}/^{184}\text{W})^{BSE}$  and  $(^{180}\text{Hf}/^{184}\text{W})^{BSE}$ ). The results of this equation for various values of  $t_d$  between 0 and 50 Myr are illustrated in Figure 1.1. This figure reveals that core-mantle segregation can only affect the  $^{182}\text{W}/^{184}\text{W}$  composition of the mantle if  $t_d < 50$  Myr. After this point in time,  $^{182}\text{Hf}$  was effectively extinct and any later Hf-W fractionation could not have led to variations in the  $^{182}\text{W}/^{184}\text{W}$  ratio between the mantle and the core.

Calculating two-stage model ages requires knowledge of the W isotopic evolution of chondrites, which is assumed to represent that of the bulk, undifferentiated planet. To calculate the Hf-W isotopic evolution of chondrites, their initial  $^{182}\text{Hf}/^{180}\text{Hf}$  and  $^{182}\text{W}/^{184}\text{W}$  compositions,  $^{180}\text{Hf}/^{184}\text{W}$  ratio and present-day W isotopic composition needs to be known (Equation (5)). The most direct approach for determining the initial Hf and W isotopic compositions of chondrites is to obtain internal Hf-W isochrons for the oldest objects formed in the solar system, the Ca,Al-rich inclusions (CAIs) found in carbonaceous chondrites. The slope of the CAI isochron does not directly provide an age, as is the case for

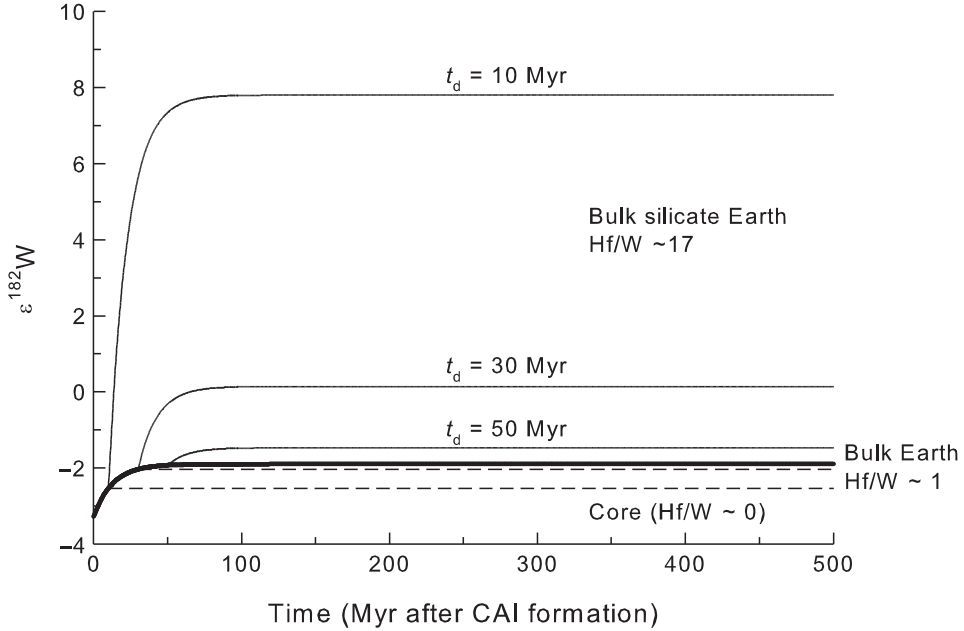


Fig. 1.1 A simple two-stage model illustrating the isotopic evolution of core and mantle reservoirs segregated at various times ( $t_d$ ) after formation of the solar system.

long-lived chronometers, but instead yields the abundance of the parent nuclide (i.e.  $^{182}\text{Hf}/^{180}\text{Hf}$ ) at the time of CAI formation. Thus, the chronology obtained from Hf-W on planetary differentiation is not absolute but is established relative to the formation of CAIs at  $t_0 = 0$ . In order to determine an absolute chronology, it is necessary to estimate independently the age of CAIs using a long-lived radioactive system. The U-Pb chronometer gives ages of  $\sim 4.568$  Gyr for CAI formation (Amelin *et al.*, 2002; Bouvier *et al.*, 2007).

An internal Hf-W isochron for mineral separates from several CAIs from the Allende and NWA 2364 CV chondrites gives the following initial values: initial  $^{182}\text{Hf}/^{180}\text{Hf} = (9.72 \pm 0.44) \times 10^{-5}$  and initial  $\epsilon^{182}\text{W} = -3.28 \pm 0.12$  (Figure 1.2). Bulk carbonaceous chondrites have a more radiogenic W isotopic composition of  $\epsilon^{182}\text{W} = -1.9 \pm 0.1$  (Kleine *et al.*, 2002, 2004a; Schoenberg *et al.*, 2002; Yin *et al.*, 2002b). Note that the first

W isotope data for chondrites, obtained by Lee & Halliday (1995), yielded  $\epsilon^{182}\text{W} \sim 0$ , but later studies showed that this initial measurement was inaccurate. The elevated  $^{182}\text{W}/^{184}\text{W}$  of chondrites compared to the initial value of the solar system reflects the decay of  $^{182}\text{Hf}$  to  $^{182}\text{W}$  over the age of the solar system, and from this difference the time-integrated  $^{180}\text{Hf}/^{184}\text{W}$  of chondrites can be calculated using Equation (5). This approach results in a time-integrated  $^{180}\text{Hf}/^{184}\text{W}$  of chondrites of 1.23, identical to the results of high-precision concentration measurements that yield an  $^{180}\text{Hf}/^{184}\text{W}$  ratio of 1.23 (Kleine *et al.*, 2004a).

Once the Hf-W isotopic evolution of chondrites is defined, two-stage model ages of core formation can be calculated from the Hf/W ratio and  $\epsilon^{182}\text{W}$  value of the mantle or core of a differentiated planetary body (Equation (9)). We will discuss these two-stage model ages for several planetary bodies in detail in the section on 'Hf-W

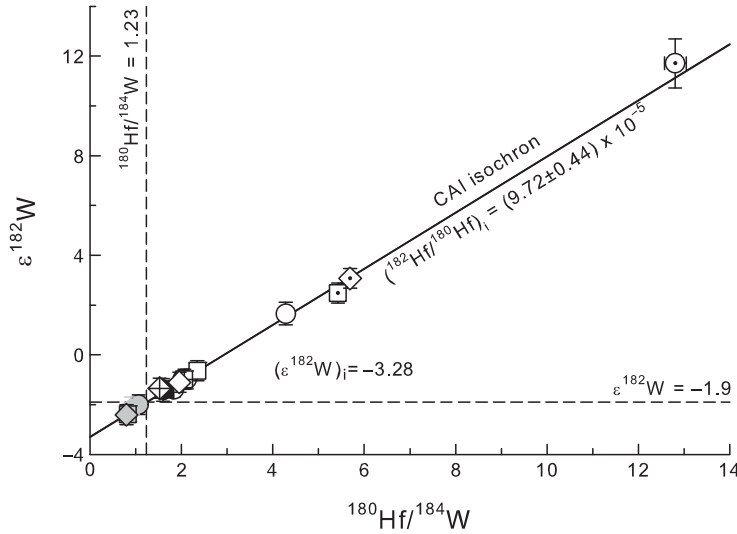


Fig. 1.2 Hf-W isochron of Ca,Al-rich inclusions from CV chondrites. Data points are for different mineral separates from CAIs. Those with the highest  $^{180}\text{Hf}/^{184}\text{W}$  and  $\epsilon^{182}\text{W}$  are for fassaites. The solar system initial Hf and W isotopic compositions are defined by the CAI isochron. Also shown with dashed lines are the Hf-W parameters for average chondrites. Modified from Burkhardt *et al.* (2008).

chronology of the accretion and early differentiation of the Earth and Moon.'

However, when considering the short half-life of  $^{182}\text{Hf}$  (9 Myr) and the characteristic timescale of accretion and core formation (10–100 Myr), it is evident that core formation cannot be treated as an instantaneous event and more complex, continuous segregation models are required. These also will be discussed in more detail in that section. The two-stage model, however, is extremely useful as it provides a maximum age for the completion of core formation.

Because both Hf and W are refractory, it has been customary to assume that their relative abundances remained more or less constant throughout the solar system. Consequently, for refractory elements, the composition of the bulk Earth must be close to that of chondrites (i.e.  $(^{180}\text{Hf}/^{184}\text{W})_{\text{BE}} = 1.23$ ). In detail, however, the composition of the bulk Earth may deviate from that of chondrites due to collisional erosion of early-formed crust (O'Neil & Palme, 2008; Warren, 2008). Due to the higher incompatibility of W compared to Hf, planetary crusts have sub-chondritic Hf/W ratios, such that impact-induced erosion of such crustal material would tend to increase the Hf/W ratio of the bulk Earth com-

pared to chondrites. Obviously this would affect the chronology derived from Hf-W systematics. This aspect and its consequences on chronological constraints derived from  $^{182}\text{Hf}$ - $^{182}\text{W}$  will be briefly discussed in later sections.

### Coupled $^{146}\text{Sm}$ - $^{142}\text{Nd}$ and $^{147}\text{Sm}$ - $^{143}\text{Nd}$ chronometry

The coupled Sm-Nd system is a chronometer composed of an extinct and an extant radioactivity:  $^{143}\text{Nd}$  is produced by  $\alpha$ -decay of the long-lived  $^{147}\text{Sm}$  ( $T_{1/2} = 106$  Gyr), and  $^{142}\text{Nd}$  was produced by  $\alpha$ -decay of now-extinct  $^{146}\text{Sm}$  ( $T_{1/2} = 103$  Myr). The domain of application of these chronometers is thus conditioned by their respective half-life and by the chemical properties of the Rare Earth Elements (REE). As with most REE, Sm and Nd are characterized by high condensation temperatures (Boynton, 1975; Davis & Grossman, 1979), moderate incompatibility during magmatic processes and an extremely lithophile behavior during metal-silicate segregation. Core formation is thus unlikely to fractionate the REE significantly, even under highly reducing conditions, whilst volatility-controlled fractionation has only been observed in high-T

**Table 1.1**  $^{147}\text{Sm}$ - $^{143}\text{Nd}$  systematics in the major terrestrial reservoirs (upper crust, depleted mantle, and bulk silicate Earth)

	$^{143}\text{Nd}/^{144}\text{Nd}$	$^{147}\text{Sm}/^{144}\text{Nd}$	Source
Upper crust	0.5116	0.117	Taylor & McLennan (1985)
Depleted mantle	0.5131	0.215–0.235	Salters & Stracke (2004)
BSE (chondritic model)	0.512638	0.1966	Jacobsen & Wasserburg (1984)
BSE (non-chondritic model)	0.51299	0.2082	Caro <i>et al.</i> (2008)

condensates such as CAIs (Ireland *et al.*, 1988). At the exception of extremely reducing nebular environments, where Samarium can be reduced to a divalent state (Lodders & Fegley, 1993; Pack *et al.*, 2004), Sm and Nd are trivalent and do not experience redox-controlled fractionation. As a consequence, the relative abundances of Sm and Nd in planetary reservoirs are essentially controlled by partial melting and fractional crystallization processes involved in the formation of planetary crusts (Table 1.1). As Nd is normally more incompatible than Sm, crustal reservoirs formed by partial melting of the mantle, or by fractional crystallization of a magma ocean, will have low Sm/Nd ratios and high Nd concentration, whilst the residual mantle reservoirs are characterized by a higher Sm/Nd (Table 1.1). Differentiated crust or mantle are thus expected to develop distinct  $^{143}\text{Nd}/^{144}\text{Nd}$  signatures, usually noted  $\epsilon^{143}\text{Nd}$ :

$$\epsilon^{143}\text{Nd} = \left( \frac{(^{143}\text{Nd}/^{144}\text{Nd})}{(^{143}\text{Nd}/^{144}\text{Nd})_{\text{CHUR}}} - 1 \right) \times 10^4 \quad (10)$$

where CHUR (Chondritic Uniform Reservoir) represents the average chondritic composition. A similar notation is used for the  $^{146}\text{Sm}$ - $^{142}\text{Nd}$  system, with  $(^{142}\text{Nd}/^{144}\text{Nd})_{\text{BSE}}$  as the normalizing ratio. Long-lived differentiated crustal reservoirs are thus expected to develop unradiogenic  $\epsilon^{143}\text{Nd}$ , whilst an elevated  $\epsilon^{143}\text{Nd}$  indicates derivation from a mantle previously depleted in incompatible elements. If differentiation takes place prior to extinction of  $^{146}\text{Sm}$  (i.e. >4.2 Gyr ago), then crustal and mantle reservoirs will also develop

distinct  $\epsilon^{142}\text{Nd}$  signatures, respectively lower and higher than the BSE composition.

The existence of distinct  $\epsilon^{143}\text{Nd}$  signatures between terrestrial silicate reservoirs (Figure 1.3) has permitted the establishment of constraints on the chronology of mantle-crust differentiation (Jacobsen & Wasserburg, 1979; Allegre *et al.*, 1979; DePaolo & Wasserburg, 1979; DePaolo, 1980), the exchange fluxes between crust and mantle (Albarede & Rouxel, 1987; Albarede, 2001) and the fate of recycled crustal material in the mantle (Zindler & Hart, 1986). However, the constraints derived from  $^{147}\text{Sm}$ - $^{143}\text{Nd}$  systematics only depict a relatively recent (<2–3 Gyr) history of the mantle-crust system. Events that took place earlier in Earth’s history are far more difficult to constrain, because their isotopic fingerprint on mantle composition has been erased by later crustal formation and recycling. In contrast, the  $^{146}\text{Sm}$ - $^{142}\text{Nd}$  chronometer is only sensitive to events that took place during the very early history of the Earth. Given the current analytical uncertainties on Nd isotopic measurements ( $2\sigma = 2$ –5 ppm), radiogenic ingrowth in silicate reservoirs becomes negligible after approximately 4 periods. Distinct  $^{142}\text{Nd}$  signatures can thus only develop in silicate reservoirs differentiated prior to 4.2 Gyr. Thus, whilst the  $^{143}\text{Nd}/^{144}\text{Nd}$  composition of modern silicate reservoirs is mainly inherited from continuous crustal formation during the past 2 to 3 Gyr, their  $^{142}\text{Nd}$  signature can only be the result of much earlier REE fractionation, thereby making the  $^{146}\text{Sm}$ - $^{142}\text{Nd}$  system a selective tool for dating the formation of the earliest crusts on Earth and other terrestrial planets.

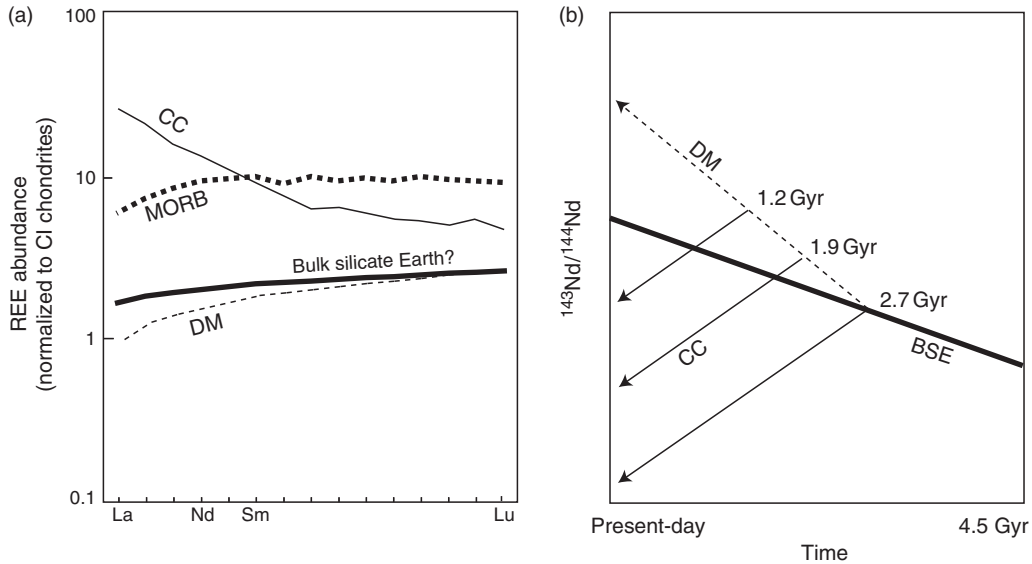


Fig. 1.3 (a) REE abundance patterns of the major terrestrial silicate reservoirs normalized to CI chondrites. The CI-normalized pattern of the bulk silicate Earth is not directly constrained but has been conservatively assumed to be perfectly flat, with  $[\text{REE}]_{\text{BSE}} = 2.75 \times [\text{REE}]_{\text{CHUR}}$  (McDonough & Sun, 1995). However, a slightly non-chondritic composition, perhaps similar to the hypothetical pattern shown here, is suggested by the non-chondritic  $^{142}\text{Nd}$  composition of terrestrial samples. A large fraction (30–50%) of the LREE budget of the silicate Earth is concentrated in the continental crust, which shows an enrichment by 1–2 orders of magnitude compared with bulk silicate Earth values. In contrast, the uppermost mantle (as sampled by mid-ocean ridge basalts) is characterized by a depleted REE pattern (LREE < HREE) and a radiogenic  $^{143}\text{Nd}/^{144}\text{Nd}$  signature indicative of long-term evolution with high Sm/Nd ratio. (b) Schematic illustration showing the  $^{143}\text{Nd}/^{144}\text{Nd}$  evolution of major silicate reservoirs. The present-day continental mass was formed during three major episodes of crustal growth at 2.7, 1.9 and 1.2 Gyr (Condie, 2000). This process extracted about one-third of the total Nd budget of the bulk Earth, creating an enriched reservoir with low  $^{147}\text{Sm}/^{144}\text{Nd}$  ratio (0.12), which subsequently evolved towards unradiogenic  $\epsilon^{143}\text{Nd}$  (–15  $\epsilon$ -units), and a complementary depleted mantle characterized by high  $^{147}\text{Sm}/^{144}\text{Nd}$  (0.23–0.25) and radiogenic  $\epsilon^{143}\text{Nd}$  signature ( $\epsilon^{143}\text{Nd} = +9$ ) (Allegre *et al.*, 1979; DePaolo & Wasserburg, 1979; Jacobsen & Wasserburg, 1979). Recycling of oceanic crust in the deep mantle may also contribute to depleting the uppermost mantle in incompatible elements (Christensen & Hofmann, 1994).

#### Two-stage mantle-crust differentiation model

The development of  $^{146}\text{Sm}$ - $^{142}\text{Nd}$  systematics has long been hampered by the difficulty of measuring with sufficient precision the small radiogenic effects on  $^{142}\text{Nd}$  (Sharma *et al.*, 1996), a problem essentially due to the scarcity of  $^{146}\text{Sm}$  in the early solar system. The presence of this p-process radionuclide was first demonstrated by Lugmair & Marti (1977), who reported radiogenic  $^{142}\text{Nd}$  effects in mineral separates from the achondrite Angra Dos Reis. This observation was then confirmed by

the discovery of highly radiogenic  $^{142}\text{Nd}$  signatures in carbon-chromite fractions from the chondrite Allende, which were attributed to  $\alpha$ -recoil effects from  $^{146}\text{Sm}$  in carbon films surrounding Sm-bearing grains (Lugmair *et al.*, 1983). In the early 1990s, accurate determinations of the initial abundance of  $^{146}\text{Sm}$  were obtained using a new generation of mass spectrometers. Lugmair & Galer (1992) reported an initial  $^{146}\text{Sm}/^{144}\text{Sm}$  ratio of  $0.0071 \pm 17$  for Angra Dos Reis and Prinzhofer *et al.* (1989, 1992) suggested a value of  $0.008 \pm 1$  from mineral separates of the meteorites Ibitira and Morristown (Figure 1.4). These estimates are in general agree-



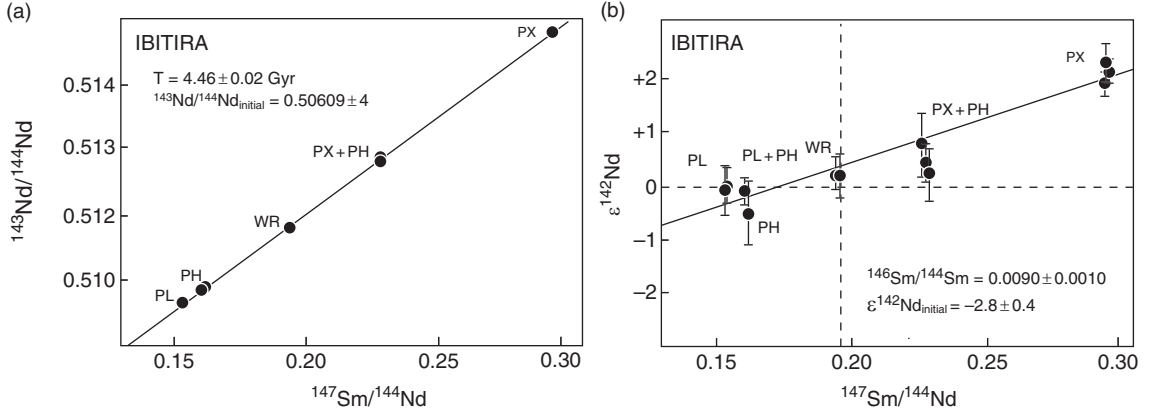


**Fig. 1.4** (a)  $^{147}\text{Sm}$ - $^{143}\text{Nd}$  and (b)  $^{146}\text{Sm}$ - $^{142}\text{Nd}$  mineral isochrons from the Euclite Ibitira (Prinzhofer *et al.*, 1992).  $^{142}\text{Nd}$  heterogeneities in mineral separates are correlated with their respective Sm/Nd ratio, demonstrating the presence of live  $^{146}\text{Sm}$  at the time of crystallization of the rock. In contrast with the long-lived  $^{147}\text{Sm}$ - $^{143}\text{Nd}$  system, the slope of the  $^{146}\text{Sm}$ - $^{142}\text{Nd}$  isochron does not yield an absolute age but is proportional to the abundance of the parent nuclide (i.e.  $^{146}\text{Sm}/^{144}\text{Sm}$ ) at the time of crystallization. Mineral isochrons established in chondrites and achondrites provide a best estimate for the initial  $^{146}\text{Sm}/^{144}\text{Sm}$  ratio of  $0.008 \pm 1$ . Reprinted from “*Geochimica et Cosmochimica Acta*”, 56:2, A Prinzhofer, D.A Papanastassiou, G.J Wasserburg, Samarium-neodymium evolution of meteorites, pp. 1–2, 1992, with permission from Elsevier.

ment with more recent results obtained by Nyquist *et al.* (1994) and Amelin & Rotenberg (2004) and were widely applied as reference parameters in later studies (Harper & Jacobsen, 1992; Caro *et al.*, 2003; Boyet & Carlson, 2005).

The two-stage model described for the  $^{182}\text{Hf}$ - $^{182}\text{W}$  chronometer can be easily transposed to mantle-crust differentiation. In this case, the two-stage model equation describing the evolution of a depleted mantle reservoir reads:

$$\left(\frac{^{142}\text{Nd}}{^{144}\text{Nd}}\right)_t^{EDM} = \left(\frac{^{142}\text{Nd}}{^{144}\text{Nd}}\right)_{t_p}^{BSE} + \frac{(^{146}\text{Sm}/^{144}\text{Sm})_{t_0}}{(^{147}\text{Sm}/^{144}\text{Sm})_{t_p}} \times \left[ \left(\frac{^{147}\text{Sm}}{^{144}\text{Nd}}\right)_{t_p}^{BSE} \times e^{-\lambda_{146}t_d} + \left(\frac{^{147}\text{Sm}}{^{144}\text{Nd}}\right)_{t_p}^{EDM} \times [e^{-\lambda_{146}t_d} - e^{-\lambda_{146}t}] \right] \quad (11)$$

where the acronyms EDM and BSE stand for Early Depleted Mantle and Bulk Silicate Earth, respectively. The term EDM is used here to avoid confusion with the modern depleted mantle, whose

chemical composition reflects continuous crustal extraction and is thus not directly relevant to early differentiation processes. Note also that in order to homogenize notations with the  $^{147}\text{Sm}$ - $^{143}\text{Nd}$  decay equation, the parent-daughter ratio in Equation (11) is often expressed as  $^{147}\text{Sm}/^{144}\text{Nd}$ .

As can be seen from Equation (11), a model age ( $t_d$ ) of mantle-crust differentiation can be derived from  $^{146}\text{Sm}$ - $^{142}\text{Nd}$  systematics, assuming that  $(^{142}\text{Nd}/^{144}\text{Nd})^{EDM}$  and  $(^{147}\text{Sm}/^{144}\text{Nd})^{EDM}$  are known. In practice, the latter cannot be estimated directly, as mantle-crust exchanges during the Archean and Proterozoic have overprinted the geochemical signature of the earlier magmatic events. However, this problem can be circumvented by combining the  $^{147}\text{Sm}$ - $^{143}\text{Nd}$  and  $^{146}\text{Sm}$ - $^{142}\text{Nd}$  systems using a simple two-stage model (Figure 1.5). The  $^{143}\text{Nd}/^{144}\text{Nd}$  evolution of the EDM can then be expressed as:

$$\left(\frac{^{143}\text{Nd}}{^{144}\text{Nd}}\right)_t^{EDM} = \left(\frac{^{143}\text{Nd}}{^{144}\text{Nd}}\right)_{t_p}^{BSE} + \left(\frac{^{147}\text{Sm}}{^{144}\text{Nd}}\right)_{t_p}^{BSE} \left[ 1 - e^{\lambda_{147}(t_p - t_d)} \right] + \left(\frac{^{147}\text{Sm}}{^{144}\text{Nd}}\right)_{t_p}^{EDM} \left[ e^{\lambda_{147}(t_p - t_d)} - e^{\lambda_{147}(t_p - t)} \right] \quad (12)$$

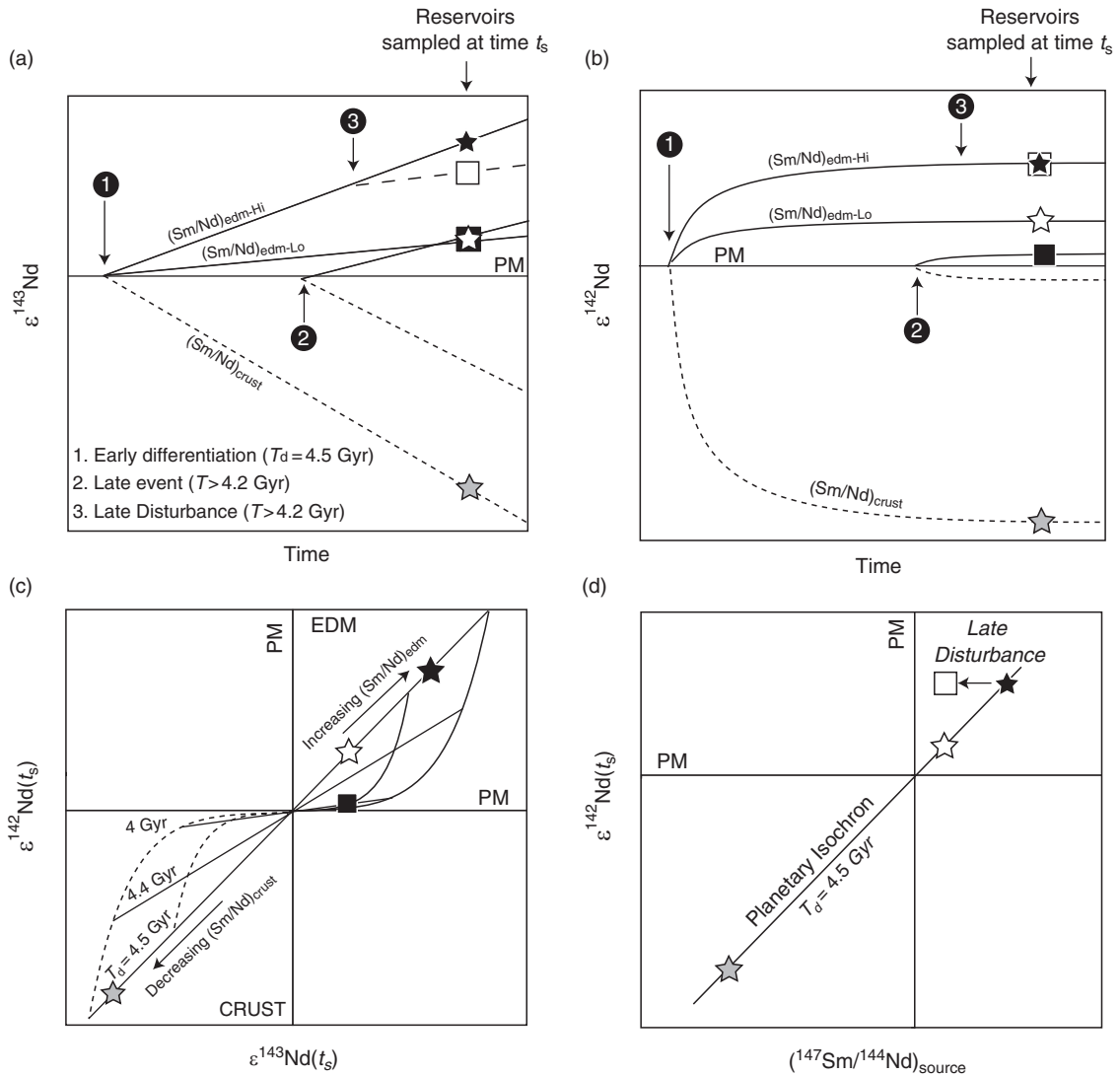


**Fig. 1.5** Schematic illustration of the coupled  $^{146,147}\text{Sm}$ - $^{142,143}\text{Nd}$  chronometer. (a)  $\epsilon^{143}\text{Nd}$  evolution of a proto-crust (labeled *crust*) and complementary mantle reservoirs (labeled *edm-Hi* and *edm-Lo*) differentiated at 4.5 Gyr (1) and 4 Gyr (2). The Archean  $^{143}\text{Nd}$  record is consistent with either a moderate  $\text{Sm/Nd}$  fractionation at a very early stage of the Earth's history (1), or more substantial fractionation at a later stage (2). (b) The  $^{146}\text{Sm}$ - $^{142}\text{Nd}$  chronometer provides more accurate chronological constraints. Here only the early event (1) can generate significant  $^{142}\text{Nd}$  excesses. In contrast, any  $\text{Sm/Nd}$  fractionation occurring after  $\sim 4.2$  Gyr would not generate significant  $^{142}\text{Nd}$  excess (2). Note that later depletion/enrichment of the EDM would modify the  $^{143}\text{Nd}/^{144}\text{Nd}$  ratio of the EDM without necessarily affecting its  $^{142}\text{Nd}/^{144}\text{Nd}$  composition (3). (c) Using coupled  $^{147}\text{Sm}$ - $^{143}\text{Nd}$  and  $^{146}\text{Sm}$ - $^{142}\text{Nd}$  chronometry, one can determine the age of differentiation of the mantle-crust system and the magnitude of  $\text{Sm/Nd}$  fractionation in the differentiated mantle (or crustal) reservoir. (d) When plotted in a  $\text{Sm/Nd}_{\text{src}}$  vs.  $\epsilon^{142}\text{Nd}_{\text{initial}}$  diagram, cogenetic reservoirs plot along a planetary isochron whose slope yields the age of differentiation of the mantle-crust system. Disturbance of this isochron relationship can occur during subsequent mantle depletion or enrichment (e.g. remelting of a magma ocean cumulate, metasomatism (3)). Note that the bulk composition of the primitive reservoir should also plot along the isochron.

where  $\lambda_{147}$  is the decay constant of  $^{147}\text{Sm}$ . By combining Equations (11) and (12), we obtain a system of two chronometric equations from which both the  $^{147}\text{Sm}/^{144}\text{Nd}$  ratio and the age of differentiation of the EDM can be calculated (Figure 1.5c). Using this coupled  $^{146,147}\text{Sm}$ - $^{142,143}\text{Nd}$  chronometer, the age of the crust can be estimated solely from its isotopic fingerprint in the mantle.

### Planetary isochrons

The two-stage model described above implies that the EDM evolved as a closed-system between  $t_d$  and  $t_s$ . However, any magmatic event affecting the EDM after 4.2 Gyr would impact the long-lived  $^{147}\text{Sm}$ - $^{143}\text{Nd}$  system without necessarily affecting the  $^{146}\text{Sm}$ - $^{142}\text{Nd}$  system (Figure 1.5a) and this could result in spurious age estimates if considered in the context of a two-stage model. A possible way of identifying such decoupling is to establish a planetary isochron (Figure 1.5d). These are constructed from a series of samples derived from cogenetic crustal and/or mantle reservoirs such as magma ocean cumulates. Although the scarcity of terrestrial samples with  $^{142}\text{Nd}$  anomalies has so far made this method inapplicable to early Earth differentiation, planetary isochrons have been used for determining ages of differentiation for the lunar and Martian mantle (see the section on  $^{146}\text{Sm}$ - $^{142}\text{Nd}$  constraints on the evolution of the Hadean crust'). In an isochron diagram, the  $^{142}\text{Nd}/^{144}\text{Nd}$  composition of samples extracted at time  $t_s$  from differentiated reservoirs are plotted against the  $^{147}\text{Sm}/^{144}\text{Nd}$  ratio of their source (Figure 1.5d). The latter are estimated using a two-stage model based on the initial  $^{143}\text{Nd}/^{144}\text{Nd}$  composition of each sample:

$$\left(\frac{^{147}\text{Sm}}{^{144}\text{Nd}}\right)_{t_p}^{\text{source}} = \frac{\left(^{143}\text{Nd}/^{144}\text{Nd}\right)_{t_d}^{\text{PM}} - \left(^{143}\text{Nd}/^{144}\text{Nd}\right)_{t_s}^{\text{source}}}{e^{\lambda_{147}t_s} - e^{\lambda_{147}t_d}} \quad (13)$$

where  $(^{143}\text{Nd}/^{144}\text{Nd})_{t_s}^{\text{source}}$  is the initial isotopic composition of a sample extracted at time  $t_s$  and  $(^{143}\text{Nd}/^{144}\text{Nd})_{t_d}^{\text{PM}}$  is the isotopic composition of the primitive mantle at  $t_d$ . An age of mantle differentiation is then obtained from the slope of the isochron (S) in an  $\epsilon^{142}\text{Nd}$  vs  $^{147}\text{Sm}/^{144}\text{Nd}$  diagram:

$$T_d = T_0 - \frac{1}{\lambda} \ln \left[ S \times \frac{\left(^{147}\text{Sm}/^{144}\text{Sm}\right)_{t_p}}{\left(^{146}\text{Sm}/^{144}\text{Sm}\right)_{t_0}} \left(\frac{^{142}\text{Nd}}{^{144}\text{Nd}}\right)_{t_p}^{\text{Std}} 10^{-4} \right] \quad (14)$$

where  $(^{142}\text{Nd}/^{144}\text{Nd})^{\text{Std}}$  is the composition of the terrestrial standard used for normalizing  $\epsilon^{142}\text{Nd}$  values. The age of differentiation is thus estimated using an iterative scheme from the slope of the regression line passing through all samples, but is not forced to intersect a hypothetical primitive mantle composition. Planetary isochrons thus provide more than simple chronological constraints. As shown in Figure 1.5d, non-cogenetic reservoirs would not plot along the same isochron, and this can be used to identify decoupling of the  $^{147}\text{Sm}$ - $^{143}\text{Nd}$  and  $^{146}\text{Sm}$ - $^{142}\text{Nd}$  systems. In addition, the position of the isochron compared with the chondritic reference provides constraints on the composition of the primitive reservoir from which planetary crusts differentiated (see the section on  $^{146}\text{Sm}$ - $^{142}\text{Nd}$  constraints on the evolution of the Hadean crust'). Ideally, cogenetic reservoirs differentiated from a primitive chondritic mantle should plot along an isochron passing through the chondritic composition (i.e. CHUR, Table 1.1). Failure to do so would indicate that the source reservoir experienced at least one additional episode of REE fractionation prior to the differentiation event recorded by the isochron. This aspect and its consequences on the composition of the terrestrial planets will be further discussed in the section on  $^{146}\text{Sm}$ - $^{142}\text{Nd}$  constraints on the evolution of the Hadean crust.'

HF-W CHRONOLOGY OF THE  
ACCRETION AND EARLY  
DIFFERENTIATION OF THE  
EARTH AND MOON

**Hf-W systematics of planetary reservoirs  
and two-stage model ages of core  
formation**

The two main parameters that need to be known to calculate Hf-W ages of core formation are the Hf/W ratio and W isotope composition of the bulk mantle or core of a planetary body. Since we do not have samples from the core and mantle of an individual planetary object, the ages are calculated relative to the composition of the bulk, undifferentiated body, which we assume to be chondritic (see section on ‘Systematics and reference parameters for short-lived radionuclides’). In the simplest model of core formation, it is assumed that the core formed instantaneously and an age for core formation can then be calculated by assuming a two-stage model (Lee & Halliday, 1995; Harper & Jacobsen, 1996; Kleine *et al.*, 2002). The underlying approach and the equation for calculating a two-stage Hf-W model age of core formation is described in detail in the section on ‘Systematics and reference parameters for short-lived radionuclides.’

The only samples available from the metallic core of differentiated planetary bodies are the magmatic iron meteorites. They contain virtually no Hf and their present-day W isotope composition is identical to that at the time of core formation (Horan *et al.*, 1998). All iron meteorites exhibit a deficit in  $^{182}\text{W}$  compared to chondrites and their  $\epsilon^{182}\text{W}$  values are among the lowest yet measured for solar system materials. Some iron meteorites even have  $\epsilon^{182}\text{W}$  values lower than the solar system initial value (as determined from Ca,Al-rich inclusions, see the section on ‘Systematics and reference parameters for short-lived radionuclides’) but these low values reflect the interaction with thermal neutrons produced during the extended exposure of iron meteoroids to cosmic rays (Kleine *et al.*, 2005a; Markowski *et al.*, 2006; Schärsten *et al.*, 2006). If these effects

**Table 1.2** Hf-W systematics of planetary reservoirs (Kleine *et al.*, 2009)

	$^{180}\text{Hf}/^{184}\text{W}$	$\epsilon^{182}\text{W}$
Chondrites	-0.6–1.8	$-1.9 \pm 0.1$
Basaltic eucrites	24–42	21–33
Angrites	4–7	1–5
Bulk silicate Mars	-3–4	$0.4 \pm 0.2$
Bulk silicate Moon	-26	$0.09 \pm 0.1$
Bulk silicate Earth	-17	$\equiv 0$

are fully taken into account, all iron meteorites have  $\epsilon^{182}\text{W}$  values indistinguishable from the initial  $\epsilon^{182}\text{W}$  of CAIs (Kleine *et al.*, 2005a; Burkhardt *et al.*, 2008). The unradiogenic  $\epsilon^{182}\text{W}$  values of iron meteorites indicate that their parent bodies differentiated within <1 Myr after formation of CAIs. Thus iron meteorites are samples from some of the oldest planetesimals that had formed in the solar system.

Hafnium-tungsten data are available for a variety of samples that derive from the silicate part of differentiated planetary bodies, including the parent bodies of some basaltic achondrites (eucrites, angrites) and Mars as well as the Earth and Moon (Table 1.2). All samples exhibit elevated Hf/W ratios and  $\epsilon^{182}\text{W}$  values compared to chondrites, indicating that Hf/W fractionation by core formation in these planetary bodies occurred during the lifetime of  $^{182}\text{Hf}$ . An important observation is that the Hf-W data for samples derived from the silicate and metal parts of differentiated planetary bodies show the pattern that is expected for Hf/W fractionation during core formation and subsequent decay of  $^{182}\text{Hf}$  to  $^{182}\text{W}$ . As such, these data confirm the basic theory of the Hf-W system as a chronometer of core formation.

Whilst determining an Hf-W age of core formation based on iron meteorite data is straightforward, because the W isotope composition of iron meteorites solely reflects Hf-W fractionation during core formation, the interpretation of Hf-W data for silicate rocks in terms of core formation timescales is more complicated. Owing to the different behavior of Hf and W during mantle

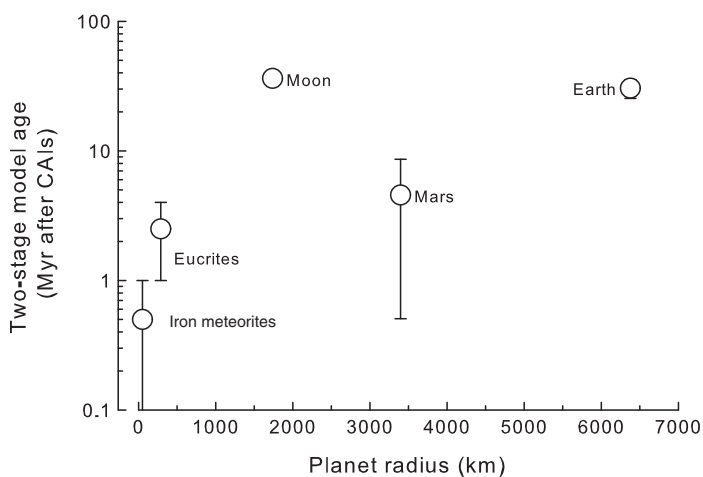


Fig. 1.6 Two-stage model age of core formation vs planet radius. After Kleine *et al.* (2002) with updated age.

melting, the Hf/W ratio of a rock is different from that of the bulk mantle of its parent body. Similarly, the W isotope composition of a mantle-derived rock may be different from that of the bulk mantle, if mantle melting occurred during the lifetime of  $^{182}\text{Hf}$ . Thus, the Hf/W ratio and W isotope composition characteristic for the entire mantle of a differentiated planetary body can often not be measured directly and the effects of Hf-W fractionation during mantle melting need to be taken into account.

Eucrites and angrites are basaltic rocks that crystallized early in solar system history near the surface of small, differentiated planetary bodies. Their Hf-W systematics were established during the early differentiation of their parent bodies and thus can be used to constrain the timing of this early differentiation. Basaltic eucrites have  $^{180}\text{Hf}/^{184}\text{W} \sim 20$  to 30 and  $\epsilon^{182}\text{W} \sim 21$  to 33 (Kleine *et al.*, 2004a; Touboul *et al.*, 2008), whilst angrites have  $^{180}\text{Hf}/^{184}\text{W} \sim 4$  to 6 and  $\epsilon^{182}\text{W} \sim 1$  to 5 (Markowski *et al.*, 2007; Kleine *et al.*, 2009). The two-stage model ages of both basaltic eucrites and angrites are similar and range from  $\sim 1$  to  $\sim 4$  Myr after CAI formation (Figure 1.6). This range in model ages is unlikely to reflect a real spread in the timing of core formation but probably is due to additional Hf-W fractionations during mantle-crust differentiation, partial melting

and, in the case of the basaltic eucrites, also thermal metamorphism.

In contrast to the basaltic achondrites, samples from Mars as well as the Earth and Moon are relatively young igneous rocks and their Hf/W ratios, which are the product of a long history of multiple melting events, are unrelated to their W isotope composition, which only reflect the earliest differentiation history of their parent bodies. The Hf/W ratio that is characteristic of the entire mantle of Mars, the Earth and the Moon can thus not be measured directly but must be determined by comparing the W concentrations in the samples with another element that behaves similarly during silicate melting (i.e. has a similar incompatibility), tends to stay in the mantle and whose abundance relative to Hf is known. The latter two conditions are met by refractory lithophile elements because their relative abundances in bulk planetary mantles should be chondritic. This is because they are neither fractionated by core formation (because they are lithophile) nor by volatile element depletion (because they are refractory). Trace element studies on Martian, lunar and terrestrial basalts show that U, Th and W have similar incompatibilities, such that the U/W or Th/W ratios of these rocks can be used to obtain an Hf/W ratio of the bulk mantle (Newsom *et al.*, 1996).

Using this approach, the following estimates for the bulk mantle Hf/W ratios are obtained:  $17 \pm 5$  (Earth),  $26 \pm 2$  (Moon) and  $3.5 \pm 0.5$  (Mars) (Kleine *et al.*, 2009).

The  $^{182}\text{W}/^{184}\text{W}$  ratios of Martian meteorites fall into two groups (Lee & Halliday, 1997; Kleine *et al.*, 2004a; Foley *et al.*, 2005b): the basaltic shergottites having  $\epsilon^{182}\text{W}$   $-0.3$  to  $0.6$  and the nakhlites and Chassigny having  $\epsilon^{182}\text{W}$   $-2$  to  $3$ . This  $^{182}\text{W}$  heterogeneity of the Martian mantle makes it difficult to estimate the  $\epsilon^{182}\text{W}$  that is characteristic for the bulk Martian mantle. Most studies have used the  $\epsilon^{182}\text{W}$  value of shergottites for the bulk Martian mantle because some shergottites have near-chondritic  $^{142}\text{Nd}/^{144}\text{Nd}$  ratios, indicating only limited trace element fractionation during early melting of their source. Using  $\epsilon^{182}\text{W} = 0.4 \pm 0.2$  and  $\text{Hf}/\text{W} = 3.5 \pm 0.5$  for the bulk Martian mantle, results in two-stage model ages of core formation of  $4.6 \pm 4.1$  Myr after CAI formation. The large uncertainty of this age largely reflects uncertainties in the mantle Hf/W ratio and the fact that this ratio is only slightly higher than the chondritic value (Nimmo & Kleine, 2007). As will be discussed in more detail below for core formation in the Earth, for larger bodies the two-stage model age does not necessarily provide a good estimate of the timescale of core formation and the two-stage model age may underestimate the time taken to accrete and differentiate Mars by a factor of  $\sim 3$  (Nimmo & Kleine, 2007). Thus, the Martian core may not have formed before  $\sim 20$  Myr after the beginning of the solar system.

In contrast to the parent bodies of basaltic achondrites and Mars, there are no  $^{182}\text{W}$  variations in the lunar and terrestrial mantles, such that the  $\epsilon^{182}\text{W}$  values of the bulk lunar mantle and the bulk silicate Earth can be measured directly and are known precisely. Determining the indigenous W isotope composition of the Moon and the extent to which  $^{182}\text{W}/^{184}\text{W}$  variations exist that reflect  $^{182}\text{Hf}$  decay within the Moon has proven to be a difficult task. There are large variations in the  $^{182}\text{W}/^{184}\text{W}$  ratios of lunar whole-rocks, which initially were interpreted to reflect an early formation of the Moon and  $^{182}\text{Hf}$ -

decay within the Moon (Lee *et al.*, 1997). More recent studies, however, showed that elevated  $^{182}\text{W}/^{184}\text{W}$  ratio in lunar whole-rocks are entirely due to the production of  $^{182}\text{Ta}$  by neutron-capture of  $^{181}\text{Ta}$  and subsequent decay of  $^{182}\text{Ta}$  to  $^{182}\text{W}$  (Kleine *et al.*, 2005b; Touboul *et al.*, 2007), and that all lunar samples have indistinguishable  $\epsilon^{182}\text{W}$  values averaging at  $0.09 \pm 0.10$  (Touboul *et al.*, 2007, 2009b). Given that lunar rocks derive from sources with highly variable Hf/W, the lack of  $^{182}\text{W}$  variations among lunar samples indicates that differentiation of the lunar mantle occurred after extinction of  $^{182}\text{Hf}$ , that is  $>60$  Myr after the beginning of the solar system. The Hf/W ratio and W isotope composition of the lunar mantle correspond to a two-stage model age of  $36 \pm 2$  Myr after CAI formation, slightly younger than the two-stage model age of the Earth's core of  $30 \pm 5$  Myr (Touboul *et al.*, 2007; Kleine *et al.*, 2009).

Figure 1.6 reveals that there is a correlation between two-stage model ages of core formation and planet size (Kleine *et al.*, 2002): the larger a planetary body, the younger is its two-stage model age. Such a pattern is unexpected if core formation did not occur until some critical stage of planetary accretion. Whilst the small meteorite parent bodies accreted early and underwent differentiation rapidly, larger bodies such as the Earth grew and differentiated over a much longer timescale. Thus, the basic assumption of the two-stage model – that is that the entire planet differentiates in one instant – is appropriate for the small meteorite parent bodies because their accretion rate is short compared to the  $^{182}\text{Hf}$  half-life. However, the two-stage model age for the Earth of  $\sim 30$  Myr indicates that accretion of the Earth occurred over a timescale that is long compared to the  $^{182}\text{Hf}$  half-life. Thus, for the Earth the assumption of instantaneous core formation is not justified, and the two-stage model time of  $\sim 30$  Myr would only date core formation if during this event the *entire* core was first remixed and homogenized with the *entire* mantle before final segregation of metal to form the present core. This is physically implausible.

The two-stage model age, therefore, is not a reasonable estimate of the exact age of the Earth's core but nevertheless provides an important constraint on the timescale of core formation. Because Hf is lithophile and W is siderophile, the bulk silicate Earth cannot have an Hf/W ratio and, hence a  $^{182}\text{W}/^{184}\text{W}$  ratio, lower than chondritic at any time, provided that the bulk Earth has chondritic relative abundances of refractory elements. Since the two-stage model assumes a chondritic W isotopic composition at the time of core formation, the calculated model age corresponds to the earliest time from which the Earth's mantle could subsequently have evolved to its present-day  $^{182}\text{W}$  excess (Halliday *et al.*, 1996; Kleine *et al.*, 2004b).

#### Hf-W isotopic evolution during continuous core formation and protracted accretion

The accretion of the Earth involved multiple collisions between smaller proto-planets. These collisions delivered the energy required for melting and core formation, such that the timescale of core formation is equivalent to the timescale of the major stage of accretion. Since the core did not segregate in a single instant at the end of accretion but formed continuously during accretion, there is no single, well-defined 'age' of core formation. An age rather corresponds to a certain growth stage of the core. A widely used model for the Earth's accretion is one that assumes an exponentially decreasing rate, such that:

$$\frac{m}{M_E}(t) = 1 - e^{-\alpha t} \quad (15)$$

where  $m/M_E$  is the cumulative fractional mass of the Earth at time  $t$  and  $\alpha$  is the time constant of accretion (Harper & Jacobsen, 1996; Jacobsen, 2005). This model provides a reasonable approximation to the Wetherill (1990) accretion model for the formation of the Earth, which is among the first of its kind. It is important to note however, that the exponential model does not mean that accretion occurred by the incremental

growth of small mass fractions. Dynamical modeling suggests that the main mass of the Earth was delivered by multiple and stochastic impacts that bring in large core masses at once (Agnor *et al.*, 1999). From the stochastic nature of these large, late-stage impacts, it follows that growth of the Earth's core occurred episodically rather than being a continuous process during accretion. The exponential model, therefore, assumes that these collisions occurred at an exponentially decreasing rate. In this model, the end of accretion is poorly constrained because accretion probably terminated with one large impact (the Moon-forming impact), the timing of which is not well defined in the exponential model. It is thus more useful to characterize the timescale in terms of a mean age of accretion,  $\tau$ , which is the inverse of the time constant  $\alpha$  and corresponds to the time taken to achieve  $\sim 63\%$  growth (cf. Harper & Jacobsen, 1996). It is also useful to characterize the timescale of the Earth's accretion by the time taken to accrete 90% of the Earth, because current models of lunar origin predict that the Moon formed during the collision of a Mars-sized impactor with a proto-Earth that was 90% accreted (Halliday, 2004, 2008; Kleine *et al.*, 2004b, 2009). Thus,  $t_{90}$  for the Earth is equivalent to the timing of the Moon-forming impact and the end of the major stage of the Earth's accretion and core formation. Using Equation (15), we show that  $t_{90} = 2.3\tau$ .

Several lines of evidence indicate that a large fraction of the Earth was accreted from objects that had already undergone core-mantle differentiation. Hafnium-tungsten data for iron meteorites and basaltic achondrites demonstrate that differentiation of their parent bodies occurred very early, within  $<1$  Myr after CAI formation (Kleine *et al.*, 2009). These data suggest that at least some of the planetesimals that accreted to the Earth were already differentiated. However, a significant amount of the Earth's mass was delivered by much larger Moon- to Mars-sized embryos. It seems inevitable that these were already differentiated prior to their collision with the proto-Earth, because models of planetary accretion predict that at 1 AU, planetary

embryos had formed within  $\sim 1$  Myr after CAI formation. In this case, they will have melted owing to heating by the decay of then abundant  $^{26}\text{Al}$ . Furthermore, planetary embryos are large enough that collisions between two embryos release sufficient energy for melting and differentiation.

A question of considerable interest for interpreting the W isotope composition of the Earth's mantle in terms of core formation timescales is the mechanism by which metal is transported to the core during the collision of a pre-differentiated object with the Earth (Harper & Jacobsen, 1996; Kleine *et al.*, 2004b, 2009; Nimmo & Agnor, 2006; Rubie *et al.*, 2007; Halliday, 2008). The key issue is if the incoming impactor metal core directly merged with the Earth's core' or finely dispersed as small droplets in the terrestrial magma ocean. In the case of *core merging*, no equilibration between the impactor core and the Earth's mantle will have taken place and the chemical and isotopic composition of the Earth's mantle would largely reflect the conditions of core formation in Earth's building blocks. In contrast, small metal droplets will have easily equilibrated with the surrounding silicate material in a magma ocean. This model, therefore, is often referred to as *magma ocean differentiation*. In this model any information on the differentiation of the impactor is lost and the chemical and isotopic composition of Earth's mantle reflects the conditions of core formation within the Earth.

Whether core merging or magma ocean differentiation is more appropriate for a given collision depends on the relative size of the two colliding bodies. Collisions in which the impactor is much smaller than the target result in vaporization of the impactor, in which case the impactor material can efficiently mix and homogenize within the magma ocean of the target. What happens in detail during larger collisions, however, is less well understood. Hydrocode simulations of giant impacts (Canup & Asphaug, 2001) show that the cores of target and impactor merge rapidly, although more recent simulations indicate that some re-equilibration

might occur (Canup, 2004). The problem is that these simulations currently provide a resolution in the order of 100 km, whereas the length-scale on which chemical and isotopic re-equilibration occurs is probably in the order of centimeters (Stevenson, 1990; Rubie *et al.*, 2007). Thus, the extent to which metal-silicate equilibration occurred during large impacts is currently not well understood.

The W isotope evolution of the Earth's mantle during accretion from pre-differentiated objects can be followed using a three-box model (Harper & Jacobsen, 1996; Halliday, 2004; Kleine *et al.*, 2004a, 2009; Jacobsen, 2005; Nimmo & Agnor, 2006). In this model, the  $^{182}\text{W}/^{184}\text{W}$  ratio of Earth's mantle immediately after addition of a new object reflects the contribution of the following three components: Earth's mantle prior to the impact (component 1); the impactor mantle (component 2); and the impactor core (component 3). We will assume that a fraction  $1-k$  of the impactor core is added directly to the target core without any prior re-equilibration with the Earth's mantle and will term  $k$  the equilibration factor ( $k = 1$  indicates complete re-equilibration). Let  $R_i$  be the  $^{182}\text{W}/^{184}\text{W}$  ratio of component  $i$  ( $i = 1, 2, 3$ ), then  $R'_1$ , the  $^{182}\text{W}/^{184}\text{W}$  ratio of the Earth's mantle immediately after the collision, is given by:

$$R'_1 = \frac{y_1 R_1 + y_2 R_2 + k y_3 R_3}{y_1 + y_2 + k y_3} \quad (16)$$

where  $y_i = m_i [\text{W}]_i$  is the total mass of W,  $m_i$  is the mass and  $[\text{W}]_i$  is the W concentration in component  $i$ .  $R_i$  for the three components at the time of the collision can be calculated using the decay equation of extinct short-lived nuclides and for the time interval between two collisions at  $t_1$  and  $t_2$  is given by:

$$R_i(t_2) = R_i(t_1) + \left( \frac{^{180}\text{Hf}}{^{184}\text{W}} \right)_i \left( \frac{^{182}\text{Hf}}{^{180}\text{Hf}} \right)_i \left( 1 - e^{-\lambda(t_2-t_1)} \right) \quad (17)$$

The total mass of W in any of these three components depends on the mass of this component and its W concentration. The latter is given by



the metal-silicate partition coefficient of  $W$ , which is defined as:

$$D^{m/s} = \frac{[W]_m}{[W]_s} \quad (18)$$

For the concentration of  $W$  in the mantle of a differentiated object, mass balance considerations and the definition of  $D$  give:

$$[W]_m = \frac{[W]_0}{D + \gamma(1 - \gamma)} \quad (19)$$

where  $[W]_0$  is the  $W$  concentration of the bulk Earth (assumed to be chondritic) and  $\gamma$  is the silicate mass fraction (in case of the Earth  $\gamma = 0.675$ ). For the concentration of  $W$  in the core we have:

$$[W]_c = \frac{[W]_0}{1 + \gamma(D - 1)} \quad (20)$$

From the equations summarized above it is clear that a number of parameters need to be known to calculate the  $W$  isotope evolution of Earth's mantle during protracted accretion with concomitant core formation. Important parameters include:

- Equilibration factor  $k$ ;
- $D$  for  $W$  in both the Earth and the differentiated objects that are accreted to form the Earth; and
- The  $^{182}\text{W}/^{184}\text{W}$  ratios in impactor mantle and core at the time of their collision with proto-Earth.

All these parameters are unknown and for the sake of simplicity, we will first assume that the metal-silicate partition coefficient  $D$  for  $W$  remained constant throughout accretion and was the same in all bodies that accreted to the Earth. We will further assume that all the bodies that collided with the Earth underwent core-mantle differentiation at  $t_0$ , the start of the solar system.

Figure 1.7 schematically illustrates the  $W$  isotope evolution of Earth's mantle in the two end-member models of metal-silicate equilibration during core formation. In the core-merging model ( $k = 0$ ), metal-silicate re-equilibration does not

occur and the  $W$  isotope composition of the target's mantle immediately after the impact results from addition of impactor mantle material to the target's mantle. The resulting  $^{182}\text{W}/^{184}\text{W}$  ratio will always be higher than chondritic because no core material (with subchondritic  $^{182}\text{W}/^{184}\text{W}$ ) is involved in these mixing processes. In the case of core merging, no isotopic record of the collision was generated and the  $W$  isotope effect in the Earth's mantle would largely reflect the timing of core formation in the pre-merged objects. In contrast, small metal droplets in a magma ocean could have equilibrated efficiently with the surrounding molten silicates. If re-equilibration was complete (i.e.  $k = 1$ ), this is equivalent to adding an undifferentiated object to the Earth's mantle, followed by metal segregation. In this case, the resulting  $W$  isotope effect reflects the rate of accretion and timing of core formation.

A variety of growth curves for the Earth's accretion, calculated by assuming an exponentially decaying accretion rate and mean times of accretion,  $\tau$  of 11, 15, and 25 Myr, are shown in Figure 1.8a. Using these growth curves and Equations (16) and (17), the  $W$  isotope evolution of the Earth's mantle can be calculated for each value of  $\tau$  and an assumed equilibration factor  $k$ . In Figure 1.8b, the  $W$  isotope evolution of Earth's mantle in the core merging and magma ocean differentiation models are compared for an assumed  $\tau$  of 11 Myr. Obviously these two models result in very different  $\epsilon^{182}\text{W}$  values for the bulk silicate Earth. The core merging model predicts highly radiogenic  $^{182}\text{W}$  in the Earth's mantle, which would reflect the timescale of core formation in the objects that later were added to the Earth (assumed to be  $t_0$ ). The magma ocean differentiation model predicts much lower  $\epsilon^{182}\text{W}$  values for the Earth's mantle, a reflection of the high degree of metal-silicate equilibration and protracted timescale of accretion in this model. Obviously, the magma ocean differentiation model is consistent with the observed  $W$  isotope composition of Earth's mantle, whilst the core merging model is not. Thus, some metal-silicate re-equilibration during accretion of the Earth from pre-differentiated objects clearly is required (Halliday *et al.*,

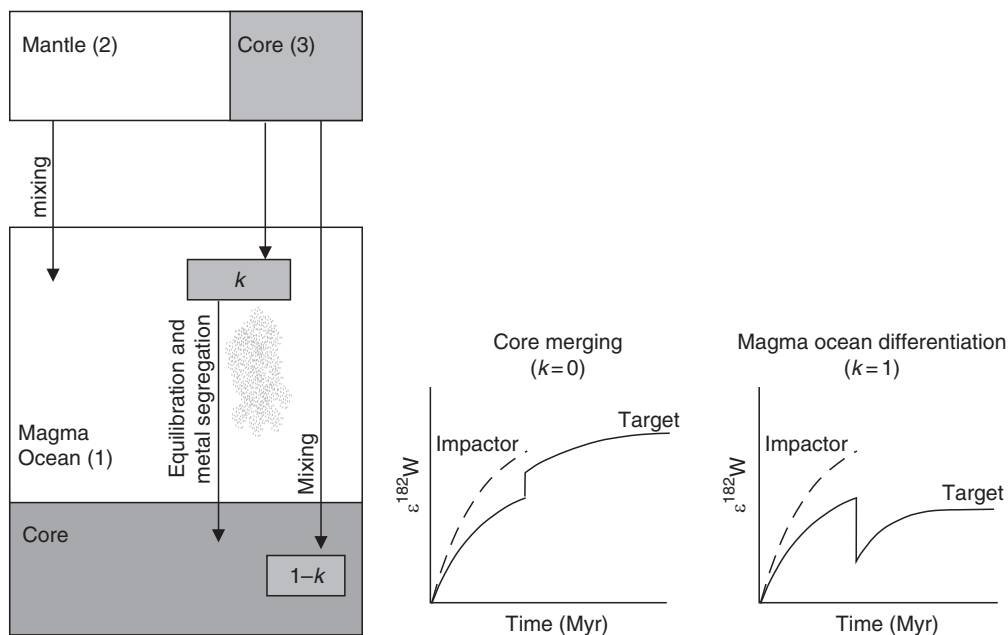


Fig. 1.7 Schematic illustration of a three-box model for W isotope evolution during protracted accretion with concomitant core formation. The components that contribute to the W isotope composition of Earth's mantle are labeled with 1, 2 and 3. The W isotope effects in the two end-member models of core formation – core merging and magma ocean differentiation – are shown schematically. Modified from Kleine *et al.* (2009).

1996; Halliday, 2004; Kleine *et al.*, 2004a, b; Jacobsen, 2005; Nimmo & Agnor, 2006).

In Figure 1.8c, W isotope evolution curves of the Earth's mantle are shown for three different combinations of  $\tau$  and  $k$ . In all three models, the present-day W isotopic composition of the Earth's mantle ( $\epsilon^{182}\text{W} = 0$ ) can be reproduced, demonstrating that determining the accretion rate of Earth ( $\tau$ ) requires knowledge of the degree to which metal-silicate re-equilibration occurred ( $k$ ). In Figure 1.9a, the calculated ages of core formation are plotted as a function of the equilibration factor  $k$ . As is evident from this figure, the calculated core formation ages become younger with decreasing values of  $k$  (Halliday, 2004; Kleine *et al.*, 2004b, 2009). Metal-silicate re-equilibration during core formation results in a decrease of the  $^{182}\text{W}$  excess in Earth's mantle that had previously accumulated due to  $^{182}\text{Hf}$  decay, such that, for a given

accretion rate, decreasing  $k$  values will result in an increasingly radiogenic W isotope composition of the Earth's mantle. Thus, to match the present-day W isotope composition of Earth's mantle, a decreasing degree of metal-silicate re-equilibration must be accompanied by longer accretion timescales, as shown in Figure 1.9a.

In all models discussed above, it was assumed that the Hf/W ratio in the mantle of the Earth, as well as all other bodies added to the Earth, was constant and identical to the present-day Hf/W ratio of the Earth's mantle. This assumption is unlikely to be valid because the metal-silicate distribution coefficient for W depends on several parameters such as pressure, temperature, and particularly oxygen fugacity (Cottrell *et al.*, 2009). These parameters are likely to have varied during accretion (Wade & Wood, 2005; Wood *et al.*, 2008). Unfortunately, there is currently little

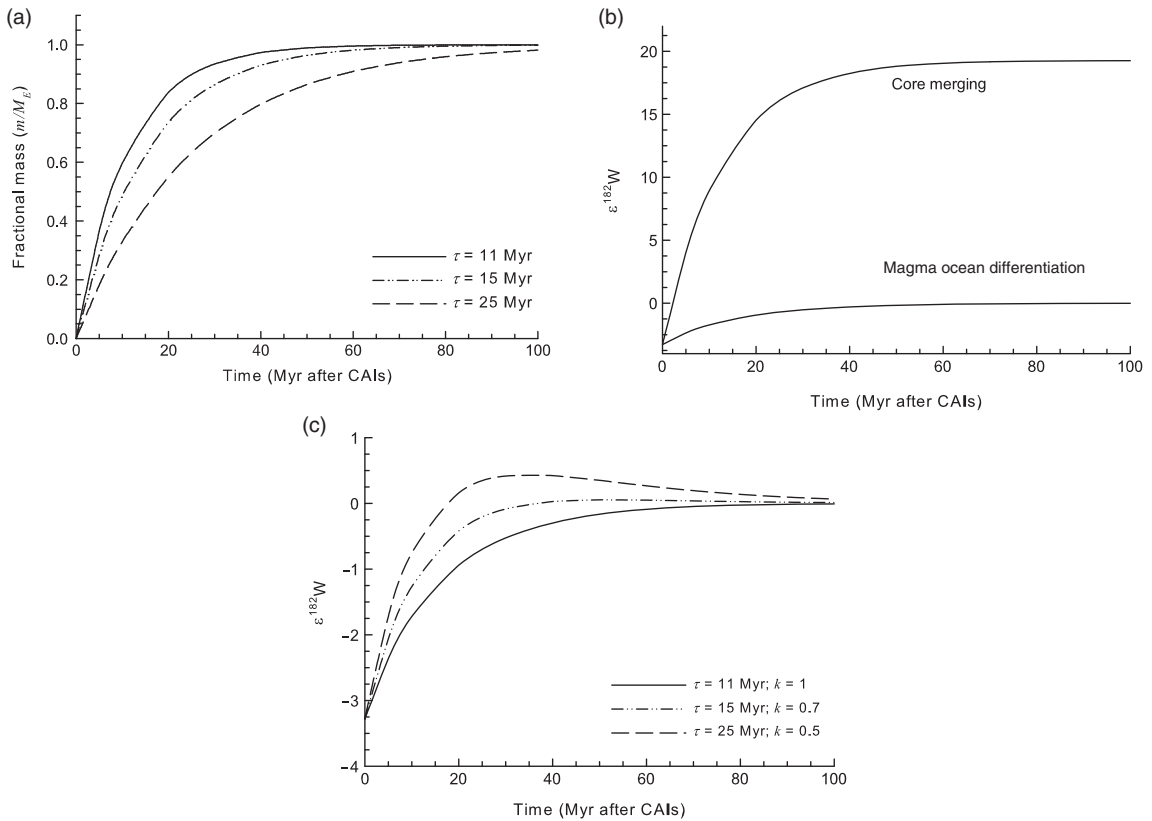


**Fig. 1.8** (a) Fractional mass of the Earth as a function of time assuming an exponentially decreasing accretion rate and a mean time of accretion of 11, 15 and 25 Myr. (b) W isotope evolution of Earth's mantle calculated for the core merging and magma ocean differentiation models, assuming a mean time of accretion of 11 Myr. (c) W isotope evolution of Earth's mantle calculated for the growth curves shown in (a) and assuming different equilibration factors  $k$ . The present-day W isotope composition of Earth's mantle ( $e^{182\text{W}} = 0$ ) can be reproduced in all three scenarios, indicating that  $\tau$  cannot be constrained independent of  $k$ .

understanding of how W partitioning into the Earth's core evolved as accretion proceeded. Most models predict that conditions were highly reducing during the early stages of accretion and became more oxidizing towards the end of accretion (Wade & Wood, 2005; Wood *et al.*, 2008). However, other models argue for the opposite (Halliday, 2004; Rubie *et al.*, 2004). In any event, the W partitioning into the core was clearly different in different planetary bodies, as is evident from the large range in Hf/W ratios in planetary mantles.

In Figure 1.9b, the calculated core formation ages are plotted against the Hf/W ratios in the impactor's mantles. In these calculations, a constant equilibration factor was assumed. This figure reveals that for a given equilibration factor (in this case  $k = 0.5$ ) decreasing Hf/W ratios in the impactor's mantles result in shorter calculated accretion rates of the Earth. The reason for this is that a mantle with a relatively low Hf/W ratio will never develop a large  $^{182}\text{W}$  excess, even if differentiation occurred very early. Consequently, for a given value of  $k$ , decreasing Hf/W ratios in

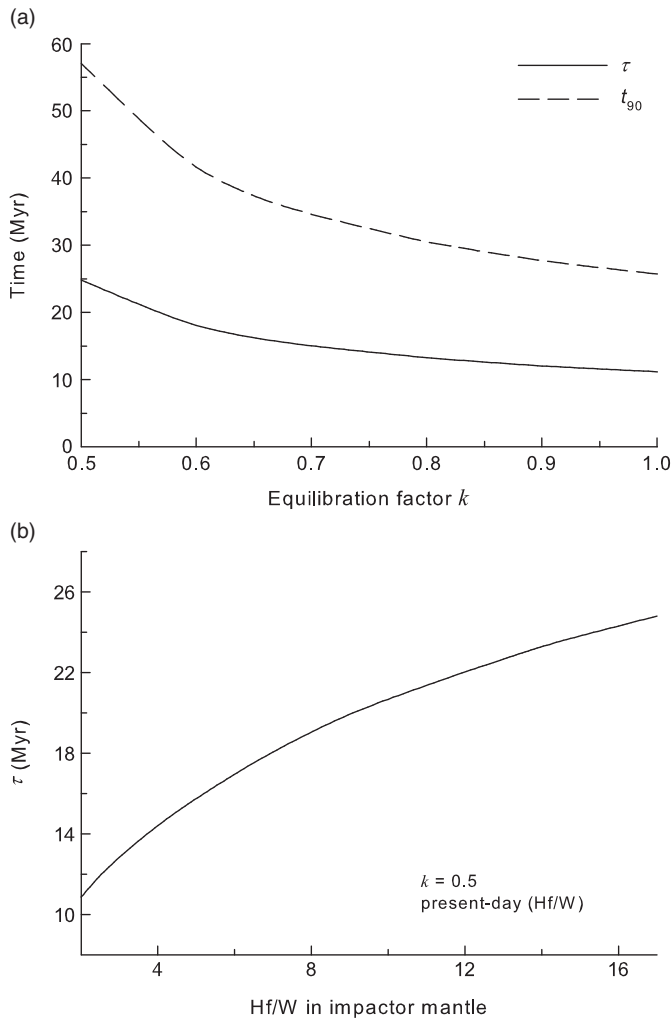


**Fig. 1.9** (a) Effect of incomplete metal-silicate equilibration on calculated core formation ages. Shown are results for the calculated value of  $\tau$  and for the time at which 90% growth was achieved (b) Effect of variable Hf/W ratios in the impactor's mantles on calculated core formation ages. In these calculations, it is assumed that the equilibration factor  $k$  was 0.5 throughout. After Kleine *et al.* (2004b; 2009).

the impactor's mantles led to less radiogenic  $^{182}\text{W}/^{184}\text{W}$  in the Earth's mantle. Thus, in such a model, the present-day W isotope composition of the Earth's mantle is reproduced by assuming a shorter accretion timescale.

In summary, determining the age of the Earth's core using the Hf-W system requires knowledge of the degree of isotopic equilibrium during metal-silicate separation, on the conditions of core formation in the growing Earth and its building blocks, and on the timescale of core formation in the planetary embryos that

were accreted to form the Earth. However, these aspects are currently not well understood, making determining the exact age of the Earth's core difficult. In spite of these uncertainties, the Hf-W data allow some important and robust conclusions to be drawn:

- The relatively small  $^{182}\text{W}$  excess found in the Earth's mantle compared to  $^{182}\text{W}$  anomalies found in eucrites and iron meteorites indicates a much more protracted timescale of accretion and core formation in the Earth compared to the smaller meteorite parent bodies;

- Core formation in the Earth can have terminated no earlier than  $\sim 30$  Myr after solar system formation, as shown by its two-stage Hf-W model age;
- Core formation in the Earth must have involved some re-equilibration of newly accreted metal within a terrestrial magma ocean, otherwise the  $^{182}\text{W}$  excess of the Earth's mantle should be one order of magnitude higher than observed. However, as discussed above, the degree to which this re-equilibration occurred is not known.

### Age of the Moon and accretion of the Earth

The models discussed in the preceding section use the present-day Hf/W ratio and W isotope composition of the Earth's mantle as the sole criterion to infer the rate at which the Earth and its core formed. We have seen, however, that the outcome of these models depends on a number of assumptions regarding the process of accretion and the conditions of core formation. Obviously, additional constraints are required and these are provided from the age and isotopic composition of the Moon. The current paradigm for the formation of the Moon is that a roughly Mars-sized body struck the proto-Earth at an oblique angle. Some fraction of the hot mantle of the impactor spun off and re-accreted outside the Roche limit to form the present-day Moon. It is widely believed that the Moon-forming impact was the last major event in the Earth's accretion, occurring when the Earth was  $\sim 90\%$  accreted (Canup & Asphaug, 2001). This giant impact caused widespread melting of the Earth's mantle and led to the final stage of core formation in the Earth (Tonks & Melosh, 1993). Thus, dating the Moon provides an independent constraint on the timescale of Earth's accretion and core formation and can be used to test the models discussed in the previous section.

Lunar samples exhibit variable and large excess in  $^{182}\text{W}$  but these W isotope variations are the result of cosmogenic  $^{182}\text{W}$  production (see above). Once these cosmogenic effects are eliminated, all lunar samples have a W isotopic composition indistinguishable from that of the Earth's man-

tle (Touboul *et al.*, 2007, 2009b). This similarity is unexpected and the currently favored explanation for this observation is the Earth and Moon isotopically equilibrated in the aftermath of the giant impact via a shared silicate atmosphere (cf. Pahlevan & Stevenson, 2007). As to whether this model is viable for equilibrating W isotopes is unclear and the alternative model to account for the similar W isotopes in the lunar and terrestrial mantles is that large parts of the Moon are derived from Earth's rather than from the impactor's mantle. This, however, is difficult to reconcile with results from dynamical models of lunar origin, all of which predict that the Moon predominantly consists of impactor mantle material (Canup, 2004). Whatever the correct interpretation, the indistinguishable W isotopic compositions of the lunar and terrestrial mantles indicate that the Earth and Moon formed in isotopic equilibrium, because it is highly unlikely that the identical W isotopic compositions evolved by coincidence (Touboul *et al.*, 2007; Kleine *et al.*, 2009).

Since the lunar and terrestrial mantles have different Hf/W ratios, they should have different  $\epsilon^{182}\text{W}$  values if formation of the Moon and the final stage of core formation in the Earth occurred whilst  $^{182}\text{Hf}$  was still extant. However, the bulk silicate Moon and Earth have indistinguishable W isotopic compositions, indicating that the Moon must have formed after  $^{182}\text{Hf}$  extinction (Touboul *et al.*, 2007, 2009b). This is quantified in Figure 1.10, where the expected  $\epsilon^{182}\text{W}$  difference between the lunar and terrestrial mantles is plotted as a function of time. The current best estimates indicate that the bulk silicate Moon has an Hf/W ratio that is  $\sim 50\%$  higher than that of the bulk silicate Earth (i.e.  $f_{\text{Hf/W}} \sim 0.5$  in Figure 1.10). In this case, the Moon must have formed  $> 50$  Myr after CAI formation. However, the uncertainties on the estimated Hf/W ratios are large and their more precise determination will be an important future task for better determining the age of the Moon.

The indistinguishable  $\epsilon^{182}\text{W}$  values of the lunar and terrestrial mantles only provide a maximum age for the formation of the Moon. Its minimum

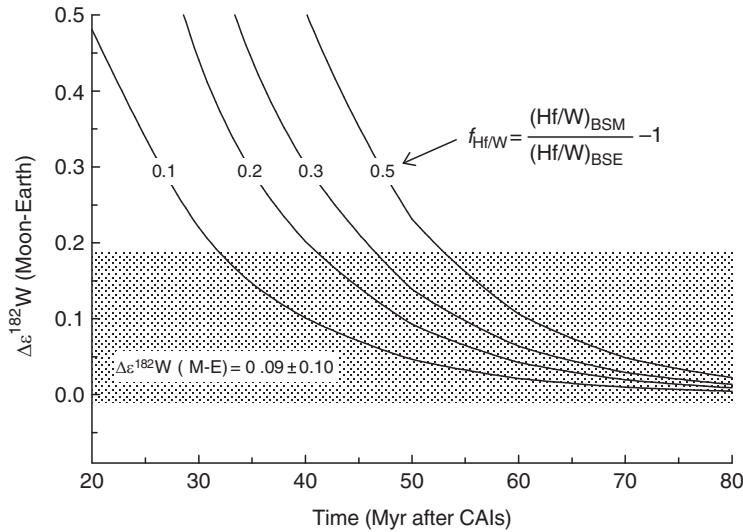


Fig. 1.10 Difference in  $\epsilon^{182}\text{W}$  values between the lunar and terrestrial mantles as a function of time (after Kleine *et al.* 2009).

age is given by the oldest lunar rocks, which are the ferroan anorthosites that have Sm-Nd ages of  $4.46 \pm 0.04$  Gyr (Carlson & Lugmair, 1988; Norman *et al.*, 2003). These two age constraints combined indicate that the Moon formed between 50 and 150 Myr after CAI formation (Touboul *et al.*, 2007, 2009b).

The age of the Moon can be used to test some of the accretion and core formation models discussed in the previous section. Two selected models, which resemble those of Halliday (2008), are shown in Figure 1.11. These were calculated by assuming that 90% of the Earth accreted at an exponentially decreasing rate and that accretion terminated by a giant Moon-forming impact at  $\sim 100$  Myr, adding the remaining 10% of the Earth's mass. The main difference between the two growth curves is that in the first model it is assumed that the Earth accreted at an exponentially decreasing rate until the giant impact at 100 Myr (Figure 1.11a), whereas in the second model 90% of the Earth was accreted rapidly within the first  $\sim 23$  Myr ( $\tau \sim 10$  Myr), followed by an accretion hiatus until the final giant impact at 100 Myr (Figure 1.11c). In both models, the present-day W isotopic composition of the bulk silicate Earth ( $\epsilon^{182}\text{W} = 0$ ) can be reproduced, but in the first model a low degree of metal-silicate

equilibration is required ( $k = 0.4$ ), whereas in the latter full equilibration occurred during core formation ( $k = 1$ ).

These two exemplary models illustrate that variable scenarios can reproduce the observed present-day Hf-W systematics of the bulk silicate Earth and the age of the Moon. An important difference between these two models is the degree to which metal-silicate equilibration occurred. Thus, constraining the degree of which equilibrium was achieved during core formation may help to distinguish among different scenarios of the Earth's accretion. The abundances of siderophile elements in the Earth's mantle may be brought to bear on this issue. They are commonly explained by metal-silicate re-equilibration under high pressures and temperatures in a deep terrestrial magma ocean (Rubie *et al.*, 2007; Wood *et al.*, 2008), in which case the model shown in Figures 1.11 c and d might best represent the Earth's accretion and core formation. However, the effects of incomplete metal-silicate equilibration on siderophile element abundances in the growing Earth have yet not been investigated and it is currently unclear as to whether they require full equilibration during core formation. Clearly, investigation of this issue will provide essential information on how the Earth accreted.

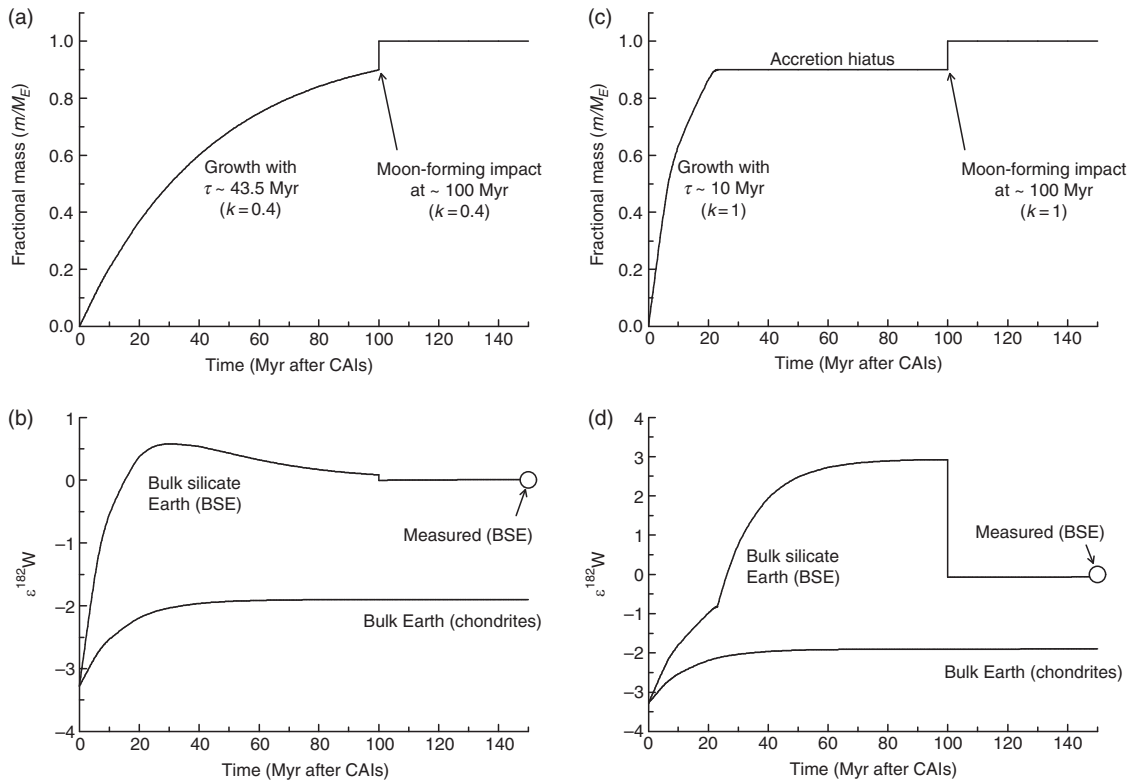


**Fig. 1.11** (a) Growth curves for the Earth assuming an exponentially decreasing accretion rate for the first 90% of growth, which was terminated by a final Moon-forming impact at  $\sim 100$  Myr that added the remaining 10% of Earth's mass. (b) W isotope evolution of the bulk silicate Earth for the growth curve shown in (a). The present-day  $\epsilon^{182}\text{W}$  of the BSE is reproduced by assuming that only 40% of the incoming impactor cores equilibrated with the Earth's mantle ( $k = 0.4$ ). (c) Growth curve for the Earth assuming an initially rapid growth with a mean life  $\tau \sim 10$  Myr, followed by an accretion hiatus and a final Moon-forming impact at  $\sim 100$  Myr. (d) W isotope evolution of the bulk silicate Earth for the growth curve shown in (c) and complete metal-silicate equilibration during core formation ( $k = 1$ ). Modified after Halliday (2008).

### $^{146,147}\text{Sm}$ - $^{142,143}\text{Nd}$ CHRONOLOGY OF MANTLE-CRUST DIFFERENTIATION ON THE EARTH, MARS, AND THE MOON

#### The $^{147}\text{Sm}$ - $^{143}\text{Nd}$ record of Archean terranes

Estimating the  $^{143}\text{Nd}$  evolution of the early Earth's mantle requires back-calculating the present-day  $^{143}\text{Nd}/^{144}\text{Nd}$  ratio of the most ancient Archean rocks at the time of their formation, in order to

obtain their initial  $\epsilon^{143}\text{Nd}$ . If the rocks are juvenile (i.e. crystallized from mantle-derived melts), then their  $\epsilon^{143}\text{Nd}_{\text{initial}}$  gives the isotopic composition of the mantle at the time of their extraction. A depleted mantle reservoir having evolved for a few hundred million years with high Sm/Nd will be characterized by positive  $\epsilon^{143}\text{Nd}$  (Figure 1.5a), whilst a primitive mantle, assuming a chondritic composition, should have  $\epsilon^{143}\text{Nd} = 0$ . Therefore, the initial isotopic composition of juvenile Archean rocks should reflect the degree of depletion of the

early Earth's mantle, and provide constraints on crustal evolution in the early Earth.

The expression used for back-calculating the present-day  $^{143}\text{Nd}/^{144}\text{Nd}$  composition of a rock sample (S) is given by:

$$\left(\frac{^{143}\text{Nd}}{^{144}\text{Nd}}\right)_{T_s} = \left(\frac{^{143}\text{Nd}}{^{144}\text{Nd}}\right)_{T_p} + \left(\frac{^{147}\text{Sm}}{^{144}\text{Nd}}\right)_{T_p} (1 - e^{-\lambda_{147}T_s}) \quad (21)$$

where  $T_s$  is age of the rock,  $T_p$  is present day, and  $T$  is time running backward from the origin of the solar system ( $T_p = 4.56$  Gyr) to the present day. Estimating initial  $^{143}\text{Nd}/^{144}\text{Nd}$  ratios thus requires the knowledge of the present-day isotopic ( $^{143}\text{Nd}/^{144}\text{Nd}$ ) $_{T_p}$  and chemical ( $^{147}\text{Sm}/^{144}\text{Nd}$ ) $_{T_p}$  composition of the rock, but also a precise estimate of its age ( $T_s$ ). The latter parameter is the most difficult to obtain, as long-lived chronometric systems in early Archean rocks are often disturbed by tectono-metamorphic events. A classic method for simultaneously estimating  $T_s$  and ( $^{143}\text{Nd}/^{144}\text{Nd}$ ) $_{T_s}$  is to establish a whole-rock  $^{147}\text{Sm}$ - $^{143}\text{Nd}$  isochron from a series of cogenetic samples (Moorbath *et al.*, 1997). In many cases, however, this method yields imprecise results due to insufficient spread in Sm/Nd, minor disturbance of the Sm-Nd system due to metamorphism, or mixing of the juvenile magmas with pre-existing crustal components. An alternative method is to independently estimate  $T_s$  using U-Pb dating of zircon grains (Bennett *et al.*, 1993). This has the advantage that U-Pb zircon ages are usually precise within a few million years, whilst whole-rock Sm-Nd isochrons have uncertainties of 50 Myr or more. This method, however, is problematic because the U-Pb age of the zircons and the Sm-Nd age of their host rock are not always identical. For example, the Acasta (Northern Canada) and Amitsôq gneisses (Western Greenland), dated at 3.6 to 4.0 Gyr and 3.73 to 3.87 Gyr using U-Pb in zircon, have younger Sm-Nd ages of 3.37 and 3.65 Gyr, respectively. Back-calculating initial  $^{143}\text{Nd}/^{144}\text{Nd}$  compositions at the zircon age thus yields highly heterogeneous  $\epsilon^{143}\text{Nd}_{\text{initial}}$  which can be incorrectly interpreted as reflecting mantle heterogeneity (Bowring & Housh, 1995; Bennett *et al.*, 1993).

Despite the difficulties in reconstructing a reliable  $^{147}\text{Sm}$ - $^{143}\text{Nd}$  record for the oldest terrestrial rocks, it is now well established that Archean terranes have initial  $^{143}\text{Nd}/^{144}\text{Nd}$  ratios more radiogenic than predicted for a primitive mantle of chondritic composition (Shirey & Hanson, 1986; Bennett, 2003) (Figure 1.12). These radiogenic signatures require that the most ancient crustal rocks were extracted from a mantle reservoir having evolved for several hundred million years with an Sm/Nd ratio 5 to 10% higher than chondritic, which has been considered as evidence that a long-lived crust formed very early (>3.8 Gyr) in the history of the Earth (Armstrong, 1981). Ancient cratons, however, represent <5% of the total mass of the present-day continents (Condie, 2000) (Figure 1.12) and this is by far insufficient to account for large-scale mantle depletion in the early Archean. It was thus suggested that Hadean continents had been recycled over shorter timescales (Armstrong, 1981; Jacobsen, 1988), or that the earliest crust was a mafic/ultramafic reservoir which, by analogy to the modern oceanic crust, did not contribute significantly to the Archean sedimentary mass (Chase & Patchett, 1988; Galer & Goldstein, 1991).

Extensive efforts to model the  $^{143}\text{Nd}$  evolution of the Archean mantle showed that the Archean  $^{147}\text{Sm}$ - $^{143}\text{Nd}$  record is consistent with a wide range of evolution scenarios for the mantle-crust system (Armstrong, 1981; Chase & Patchett, 1988; Jacobsen, 1988; Galer & Goldstein, 1991; Boyet & Carlson, 2006; Caro *et al.*, 2006). The radiogenic  $\epsilon^{143}\text{Nd}$  signature of +1 to +3  $\epsilon$ -units characterizing the early Archean mantle could, for example, result from very early (4.5 Gyr) depletion, due to magma ocean crystallization (Caro *et al.*, 2005), or from later Sm/Nd fractionation resulting from continuous crustal formation during the Hadean (Jacobsen, 1988). This ambiguity is due to the very long half-life of  $^{147}\text{Sm}$ , which limits the chronological resolution of this system (Figure 1.5a), and also to the lack of an isotopic record prior to 3.8 Gyr. In addition, the interpretation of  $^{147}\text{Sm}$ - $^{143}\text{Nd}$  data is tied to the assumption that the bulk silicate Earth has a



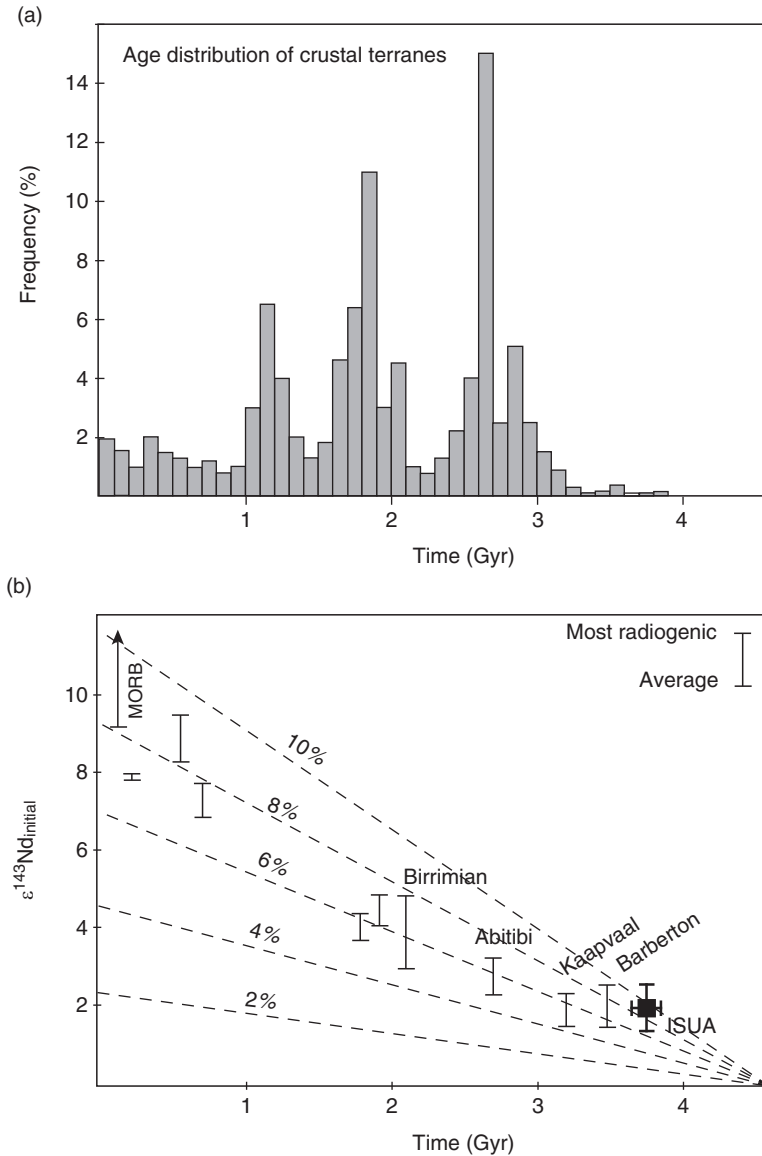


Fig. 1.12 (a) Histogram showing the age distribution of continental terranes. This distribution is characterized by three peaks of growth centered at 2.7, 1.9 and 1.2 Gyr and by a negligible amount of pre-3 Gyr crust. Reprinted from "Tectonophysics", 322: 1-2, Kent C. Condie, Episodic continental growth models: afterthoughts and extension, 2000, with permission from Elsevier. (b)  $\epsilon^{143}\text{Nd}$  evolution of the upper mantle estimated from the isotopic composition of mafic and ultramafic rocks through time. Positive  $\epsilon^{143}\text{Nd}_{\text{initial}}$  compositions are observed as far back as 3.8 Gyr, indicating that the mantle has evolved for most of its history with an Sm/Nd ratio at least 4 to 6% higher than chondritic, which cannot be explained by extraction of the present-day continents. The more radiogenic  $\epsilon^{143}\text{Nd}_{\text{initial}}$  recorded by Proterozoic juvenile rocks and modern mid-ocean ridge basalts indicates that the Proterozoic upper mantle was more depleted than the Archean mantle. This additional depletion can be explained by extraction and stabilization of large continental masses in the late Archean and Proterozoic.

perfectly chondritic composition. However, positive  $\epsilon^{143}\text{Nd}_{\text{initial}}$  may also reflect a slightly non-chondritic Sm/Nd ratio for the bulk Earth, in which case no early crustal extraction would be needed to account for the seemingly depleted signature of the Archean mantle. Thus, whilst a

realistic model of early mantle-crust evolution should always be consistent with the  $^{147}\text{Sm}$ - $^{143}\text{Nd}$  record, the chronology and mechanisms of early mantle depletion cannot be unambiguously constrained from the observed  $\epsilon^{143}\text{Nd}_{\text{initial}}$  in the Archean mantle.

### The terrestrial $^{146}\text{Sm}$ - $^{142}\text{Nd}$ record

Because of its short half-life, the  $^{146}\text{Sm}$ - $^{142}\text{Nd}$  chronometer was expected to provide more precise chronological constraints on early mantle-crust evolution. It was also anticipated that the  $^{142}\text{Nd}$  signature of early Archean rocks would be less sensitive to metamorphic disturbance than their  $^{143}\text{Nd}/^{144}\text{Nd}$  signature, owing to the negligible production rate of  $^{142}\text{Nd}$  after 4.2 Gyr. Consequently, the first searches for  $^{142}\text{Nd}$  anomalies focused on early Archean rocks from West Greenland characterized by large positive  $\epsilon^{143}\text{Nd}_{\text{initial}}$  (Goldstein & Galer, 1992; Harper & Jacobsen, 1992; Sharma *et al.*, 1996). However, these first attempts were seriously hampered by the limited precision achievable using thermal-ionization mass spectrometry (i.e.  $2\sigma$ -20 ppm). Harper & Jacobsen (1992) first reported a +33 ppm anomaly in a metasediment sample from the 3.8-Gyr-old Isua Greenstone Belt (West Greenland) but this discovery was met with skepticism as an in-depth investigation of the precision limits of thermal ionization mass spectrometers suggested that the precision quoted by the authors was perhaps overestimated (Sharma *et al.*, 1996). In addition, several studies failed to detect  $^{142}\text{Nd}$  anomalies in early Archean rocks, including samples from the Isua Greenstone Belt (Goldstein & Galer, 1992; McCulloch & Bennett, 1993; Regelous & Collerson, 1996).

With the advent of more precise thermal-ionization mass spectrometers in the last decade, it became possible to achieve precisions better than 5 ppm ( $2\sigma$ ) on the  $^{142}\text{Nd}/^{144}\text{Nd}$  ratio (Caro *et al.*, 2003, 2006). This led to the discovery of ubiquitous  $^{142}\text{Nd}$  anomalies in a series of 3.75-Gyr-old metasediments from the Isua Greenstone belt (Caro *et al.*, 2003). Similar effects were also found in Isua metabasalts and in virtually all 3.6- to 3.8-Gyr-old gneisses from the West Greenland craton (Caro *et al.*, 2006). These positive anomalies (Figure 1.13) typically ranging from 5 to 20 ppm are thus significantly smaller than the 30 to 40 ppm effects initially reported by Harper & Jacobsen (1992) and later on by Boyet *et al.* (2004) using ICP-MS technique. However, the magni-

tude of the effects reported by Caro *et al.* (2003, 2006) was confirmed by Boyet & Carlson (2005) and Bennett *et al.* (2007). In addition, Bennett *et al.* (2007) reported hints of a positive  $^{142}\text{Nd}$  anomaly in Early Archean rocks from the Narryer gneiss complex (Western Australia).

There is no ambiguity in the presence of positive  $^{142}\text{Nd}$  effects in West Greenland rocks. This depleted signature is consistent with the radiogenic  $\epsilon^{143}\text{Nd}_{\text{initial}}$  characterizing these rocks (Figure 1.12b), and indicates that this ancient craton was extracted from a reservoir depleted by crustal extraction processes >4.2 Gyr ago. As illustrated in Figure 1.14, this chronology can be further refined using coupled  $^{146,147}\text{Sm}$ - $^{142,143}\text{Nd}$  systematics (see the section on 'Coupled  $^{146}\text{Sm}$ - $^{142}\text{Nd}$  and  $^{147}\text{Sm}$ - $^{143}\text{Nd}$  chronometry').  $^{147}\text{Sm}$ - $^{143}\text{Nd}$  investigations of the metasedimentary samples studied by Caro *et al.* (2003) yielded a whole-rock isochron age of 3.75 Gyr (Moorbath *et al.*, 1997), consistent with U-Pb zircon ages from associated sedimentary formations (3.7-3.8 Gyr). This was considered as evidence that  $^{147}\text{Sm}$ - $^{143}\text{Nd}$  systematics in these samples had not been significantly disturbed by metamorphism on a whole-rock scale. The  $\epsilon^{143}\text{Nd}_{\text{initial}}$  of  $+1.9 \pm 0.6$   $\epsilon$ -units derived from this isochron was thus considered as a reliable estimate of the signature of mantle depletion characterizing the early Archean mantle. Application of coupled  $^{146,147}\text{Sm}$ - $^{142,143}\text{Nd}$  chronometry using  $\epsilon^{143}\text{Nd} = +1.9$   $\epsilon$ -units and  $\epsilon^{142}\text{Nd} = 7$  to 15 ppm yield an age of differentiation of <100 Myr (i.e.  $T_d < 4.45$  Gyr; Figure 1.14) and this age range can be narrowed to 30 to 100 Myr if we assume that the extraction of a long-lived crust must postdate core formation. The presence of positive  $^{142}\text{Nd}$  effects in the early Archean mantle thus represents strong evidence that a crustal reservoir formed at a very early stage of the Earth's history, perhaps immediately following the end of terrestrial accretion and solidification of the terrestrial magma ocean (Caro *et al.*, 2005). Together with constraints from Hf-W (see the section on 'Hf-W chronology of the accretion and early differentiation of the Earth and Moon') and Pu-I-Xe chronometers (Staudacher & Allegre, 1982; Ozima & Podosek,

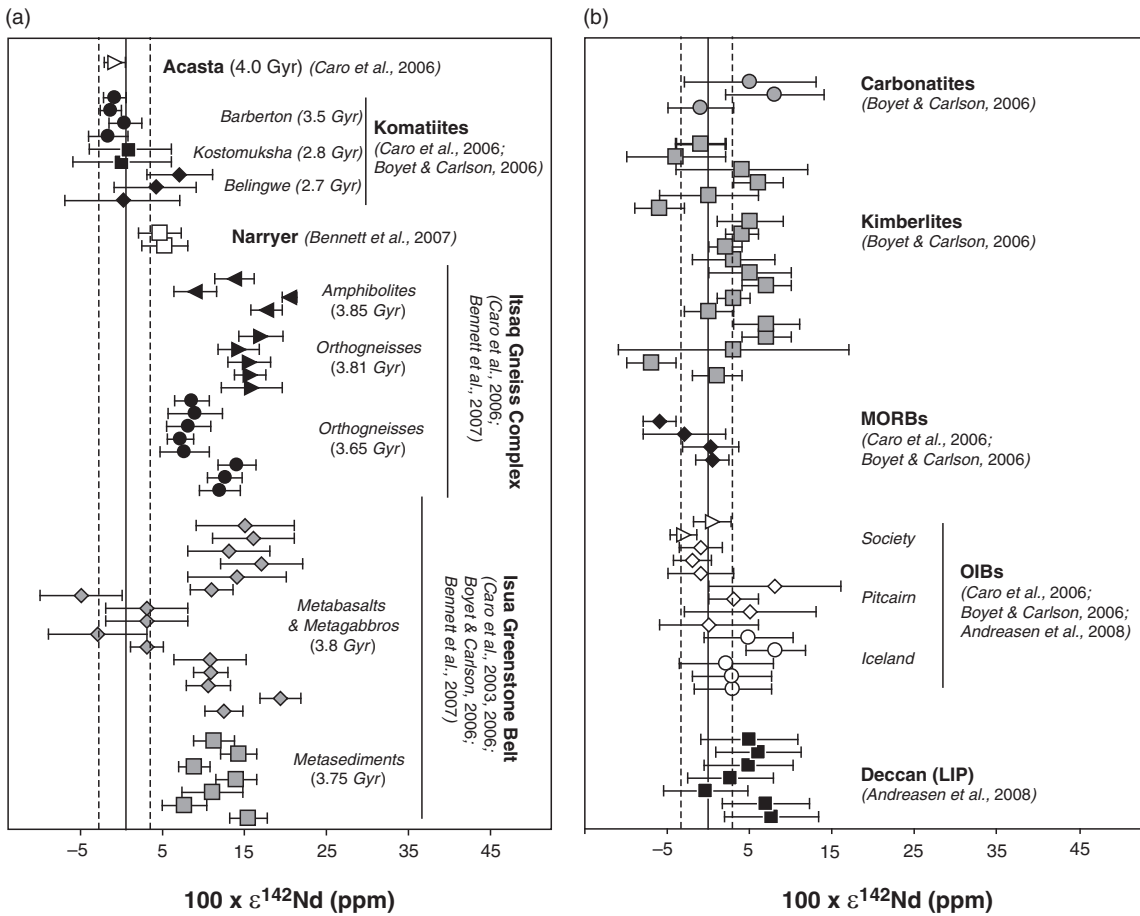


**Fig. 1.13** Compilation of high-precision  $^{142}\text{Nd}$  measurements in (a) Archean and (b) modern or recent mantle-derived rocks. The homogeneity of the modern mantle suggests that heterogeneities generated in the Hadean mantle have been efficiently remixed by mantle convection. A remnant of this ancient crust may have been preserved within early Archean cratonic roots, as suggested by negative  $^{142}\text{Nd}$  effects observed in the NSB greenstone belt and in younger rocks from the Khariar craton (O'Neil *et al.*, 2008; Upadhyay *et al.*, 2009).

1999), these results indicate that the Earth was completely differentiated with a core, an atmosphere and long-lived silicate reservoirs <100 Myr after formation of the solar system.

#### $^{146}\text{Sm}$ - $^{142}\text{Nd}$ constraints on the evolution of the Hadean crust

A proto-crust formed >4.45 Gyr ago would have developed a negative  $^{142}\text{Nd}$  anomaly of 0.5 to 1

$\epsilon$ -units, depending on its exact age and composition. Thus, even a moderate contribution of this ancient crustal material to modern magmatism would result in negative  $^{142}\text{Nd}$  effects, which should be detectable at the level of precision currently reached by mass spectrometers (Bourdon *et al.*, 2008). However, negative  $^{142}\text{Nd}$  anomalies have so far only been identified in early Archean rocks from the Nuvvuagittuq Supracrustal Belt (3.8 Gyr, Northern Canada) and in Proterozoic

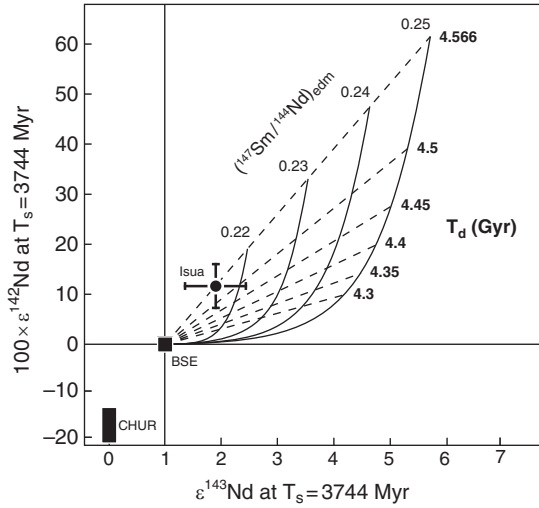


Fig. 1.14 Calculation of a model age of crustal extraction using coupled  $^{142}\text{Nd}$ - $^{143}\text{Nd}$  systematics in early Archean rocks from West Greenland. This model age was estimated by assuming a super-chondritic  $^{147}\text{Sm}/^{144}\text{Nd} = 0.2082$  for the BSE (see the section on  $^{146}\text{Sm}$ - $^{142}\text{Nd}$  constraints on the evolution of the Hadean crust'). A slightly younger model age (50–200 Myr) would be obtained by assuming differentiation from a perfectly chondritic bulk silicate Earth (Caro *et al.*, 2006).

syenites intruding the early Archean Khariar craton (<3.85 Gyr; India) (O'Neil *et al.*, 2008; Upadhyay *et al.*, 2009). If confirmed, these preliminary results would indicate that >4.2 Gyr old crust was reworked within early Archean terranes, where it was locally preserved from erosion and recycling. There is currently no evidence that such ancient crustal components were also incorporated within younger cratons, or that Hadean terranes represent a significant reservoir on a global scale. Analyses of modern mantle-derived rocks (OIBs, kimberlites, MORBs, LIPs) have also failed to provide evidence for a preserved Hadean crustal component in the mantle (Figure 1.13a), indicating that mantle heterogeneity is not inherited from early differentiation processes. Overall, these observations suggest that most of the Hadean crust was recycled and remixed within the mantle prior to the major epi-

sodes of crustal growth, making it unlikely that a large Hadean crustal reservoir was preserved until the present day.

As  $^{142}\text{Nd}$  anomalies can only be generated prior to 4.2 Gyr, their preservation in the early Archean mantle depends on the rate at which the Hadean crust was recycled and remixed in the EDM. Based on this observation, Caro *et al.* (2006) presented a simplified mantle-crust model aimed at providing a first-order estimate of the lifetime of the Hadean crust. The central postulate of this model is that the positive anomalies measured in West Greenland rocks are representative of the early Archean mantle and represent the diluted signature of a reservoir differentiated 4.5 Gyr ago. In contrast to the two-stage model presented in previous sections, the proto-crust is progressively recycled and continuously replaced by an equal volume of juvenile crust (Figure 1.15). Radiogenic mantle material is thus remixed with non-radiogenic crustal components at a rate that depends on the residence time of Nd in the crustal reservoir (i.e. the lifetime of the crust). For the sake of simplicity, it was assumed that no significant crustal growth occurs during this period, so that the mass of crust and its chemical composition remain constant. The mass transport equation for this model thus reads:

$$\frac{dM_c}{dt} = \frac{dM_m}{dt} = J_{m \rightarrow c} - J_{c \rightarrow m} = 0 \quad (22)$$

where the subscripts  $m$  and  $c$  stand for mantle and crust, respectively.  $M_i$  is the mass of the reservoir  $i$  and  $J_{i \rightarrow j}$  is the mass flux from reservoir  $i$  towards reservoir  $j$ . Equations describing the isotopic evolution of the mantle-crust system in this simple two-box model can be found in Albaredo (1995) and Caro *et al.* (2006).

Figure 1.16 shows the possible isotopic evolution curves for the early crust and its complementary depleted mantle as a function of the lifetime of the crustal reservoir  $R_c$ . The results are dependant on crustal composition, and we have therefore contrasted two different scenarios (basaltic vs continental crust), whose parameters are summarized in Table 1.3. Several constraints

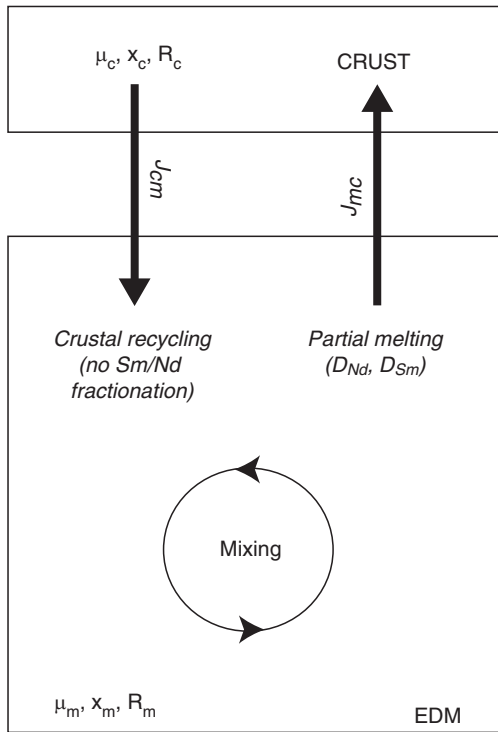


Fig. 1.15 A simplified two-box model describing a continuously interacting mantle-crust system.

on Hadean crustal dynamics can be obtained from Figure 1.16. First, it is unlikely that the Hadean crust had a lifetime shorter than 400 Myr. In this case,  $^{142}\text{Nd}$  anomalies in the mantle would be erased prior to the formation of early Archean cratons, leaving virtually no residual imprint of the earliest crust in the 3.6 to 3.8 Gyr mantle. As shown in Figure 1.16, both the basaltic and continental crust models provide a satisfying fit to the  $\epsilon^{142}\text{Nd}$  composition of the Archean mantle for significantly longer crustal residence times. In the basaltic crust model, a best fit to the early Archean mantle is obtained for values of  $R_c$  between 700 and 1,500 Myr. This value is essentially unchanged if we consider the continental crust model ( $R_c = 1\text{--}2$  Gyr). A major difference between these two case scenarios, however, lies in the preservation of  $^{142}\text{Nd}$  heterogeneities in the mantle-crust sys-

tem. In the basaltic crust model,  $^{142}\text{Nd}$  anomalies in the mantle and crust become negligible after 3.5 Gyr. Only the early Archean terranes (3.6–3.8 Gyr) would then be expected to show  $^{142}\text{Nd}$  effects. In the continental crust model,  $^{142}\text{Nd}$  anomalies are preserved over a significantly longer period of time and could be found in rocks as young as 2.5 Gyr. There is currently not enough data to decide the matter. However, the study of late Archean Greenstone Belts could provide important information regarding the lifetime and composition of the early Earth's crust.

There is currently a very limited  $^{142}\text{Nd}$  database for late Archean rocks, only including two komatiites and one carbonatite (Figure 1.13), which do not show any  $^{142}\text{Nd}$  effect at the  $\pm 10$  ppm level of precision (Boyet & Carlson, 2006). However, further examination of  $^{146}\text{Sm}\text{--}^{142}\text{Nd}$  systematics in Archean samples is needed in order to better constrain the evolution and composition of the terrestrial protocrust. If confirmed, the lack of  $^{142}\text{Nd}$  heterogeneities in the late Archean mantle-crust system could indicate that the Hadean proto-crust was more mafic than the present-day continents, and was characterized by a shorter lifetime (Figure 1.16a). This Hadean proto-crust would have been extensively recycled prior 3 Gyr, thereby making only a marginal contribution to the oldest continental cratons.

#### $^{146}\text{Sm}\text{--}^{142}\text{Nd}$ systematics of chondrites

Early studies of  $^{142,143}\text{Nd}$  systematics in planetary material have relied on two important assumptions regarding the bulk composition of the terrestrial planets. It was first assumed that these planets have perfectly chondritic Sm/Nd and  $^{143}\text{Nd}/^{144}\text{Nd}$  ratios (i.e. the CHUR reference parameters (Table 1.1)). This general paradigm follows from the observation that chondrites have a homogeneous Sm/Nd ratio (Jacobsen & Wasserburg, 1984; Patchett *et al.*, 2004; Carlson *et al.*, 2007), which is also indistinguishable (within  $\pm 10\%$ ) from the composition of the solar photosphere (Asplund *et al.*, 2006). This, in turn, suggests that high-T processes that took place in the solar nebula had a negligible effect on the REE

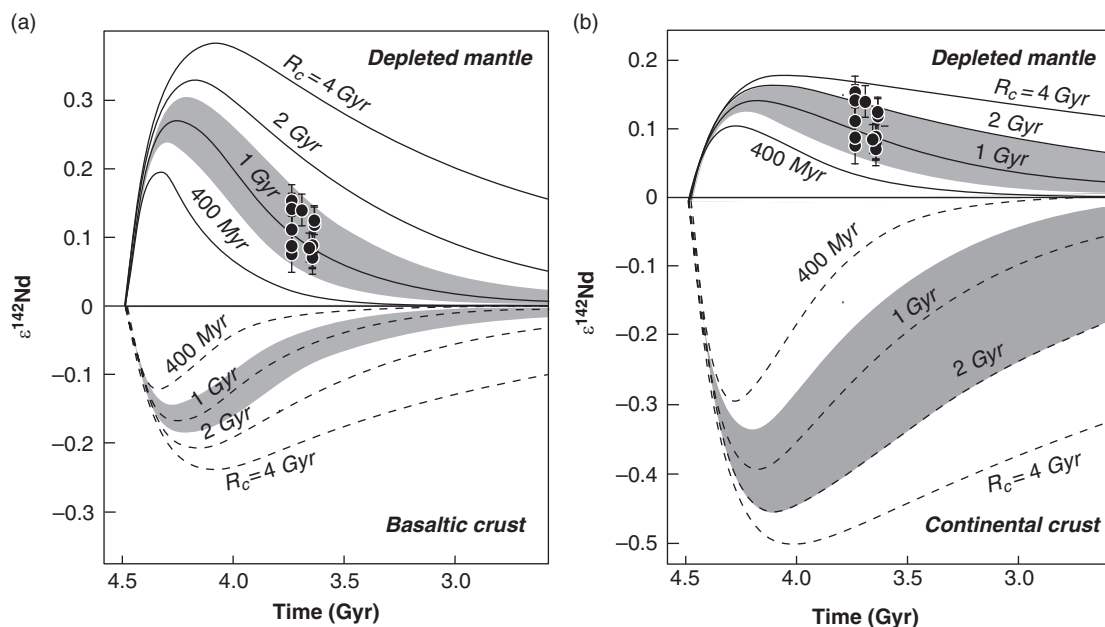


Fig. 1.16  $\epsilon^{142}\text{Nd}$  evolution of crustal and mantle reservoirs corresponding to the two-box model schematized in Figure 1.15. The curves are parameterized as a function of the crustal residence time ( $R_c$ ). The model was investigated for different crustal composition models: (a) basaltic crust and (b) continental crust. Data from Caro *et al.* (2006) and Bennett *et al.* (2007)

Table 1.3 Parameters used for modeling the  $^{146}\text{Sm}$ - $^{142}\text{Nd}$  evolution of the early depleted mantle and crust. The Aggregate melt fraction ( $F$ ) and partition coefficients ( $D_i$ ) for the continental crust model are from Hofmann (1988) and those for the basaltic crust model are from Chase & Patchett (1988). Using these parameters, one can determine the mass fraction of Nd contained in the crustal reservoir ( $x_c$ ) and the concentration of Sm and Nd in the crust and depleted mantle. The corresponding isotopic evolution of  $^{142}\text{Nd}/^{144}\text{Nd}$  in the mantle-crust system are shown in Figure 1.16.

	Continental crust model	Basaltic crust model
$F$	1.6%	5%
$D^{\text{Sm}}$	0.09	0.05
$D^{\text{Nd}}$	0.045	0.03
$x_c$	27%	64%
$[\text{Nd}]_c$ (ppm)	20	15
$[\text{Nd}]_m$ (ppm)	0.9	0.5
$(^{147}\text{Sm}/^{144}\text{Nd})_c$	0.117	0.1583

composition of the chondrite parent bodies and, by extension, on the composition of the terrestrial planets (Allegre *et al.*, 1979; DePaolo & Wasserburg, 1979; DePaolo, 1980). A second assumption is that the homogeneous  $^{142}\text{Nd}$  composition of the modern mantle and crust is representative of that of the bulk silicate Earth, from which it follows that early differentiated crustal and mantle reservoirs must have been extensively remixed over the past 4.5 Gyr (see previous section). These assumptions, however, were recently challenged by high precision studies of meteorites, showing that the chondritic  $^{142}\text{Nd}/^{144}\text{Nd}$  composition differ from that of all terrestrial samples by  $\sim 20$  ppm (Figure 1.17a) (Boyet & Carlson, 2005; Andreasen & Sharma, 2006; Carlson *et al.*, 2007). In detail, ordinary chondrites are characterized by a homogeneous composition of  $-18 \pm 5$  ppm ( $2\sigma$ , 1 data excluded), whilst carbonaceous chondrites have more negative and also more heterogeneous

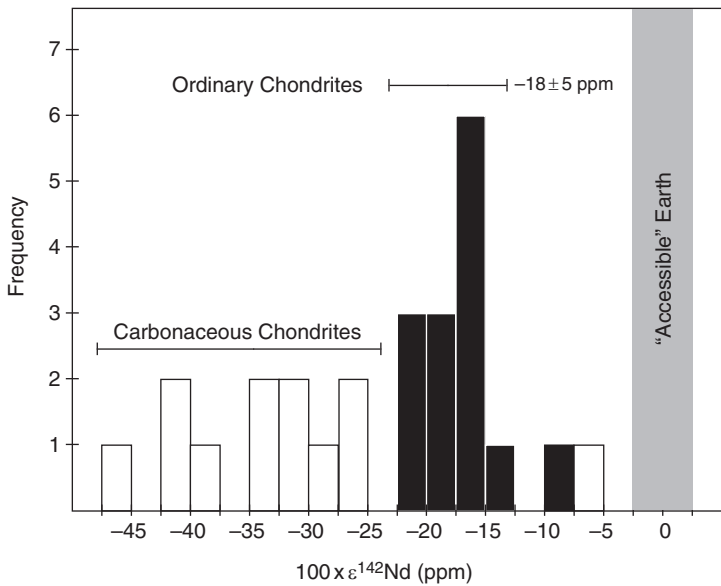


Fig. 1.17 Histogram showing the  $^{142}\text{Nd}$  composition of ordinary and carbonaceous chondrites, normalized to a terrestrial standard. Ordinary chondrites display a homogeneous composition of  $-18 \pm 5$  ppm ( $2\sigma$ ), whilst carbonaceous chondrites have more negative and also more heterogeneous signatures. Data from Boyet & Carlson (2005), Andreasen & Sharma (2006) and Carlson *et al.* (2007).

compositions ranging between  $-20$  and  $-45$  ppm. The difference between O- and C-chondrites can be explained by a heterogeneous distribution of  $^{142}\text{Nd}$  and  $^{146}\text{Sm}$  in the early solar system, resulting from incomplete mixing of nucleosynthetic products in the solar nebula (Andreasen & Sharma, 2006; Ranen & Jacobsen, 2006; Carlson *et al.*, 2007). This is best illustrated by the anomalous isotopic abundances observed for heavy elements such as Ba, Os, and Sm in C-chondrites (Carlson *et al.*, 2007; Dauphas *et al.*, 2002; Yin *et al.*, 2002a; Brandon *et al.*, 2005; Andreasen & Sharma, 2006; Ranen & Jacobsen, 2006; Reisberg *et al.*, 2009), which define a patterns similar to those observed in 'FUN' inclusion EK-141 (see review by Birck (2004)). In contrast, ordinary chondrites show normal isotopic abundances for these elements, making it more difficult to argue for a nucleosynthetic origin of the negative  $^{142}\text{Nd}$  anomalies recorded in these meteorites. It was thus proposed that the  $^{142}\text{Nd}$  excess measured in all terrestrial samples compared with ordinary chondrites result from radioactive decay in silicate reservoirs with non-chondritic Sm/Nd ratio, whilst the more negative and more heterogeneous compositions observed in carbonaceous

chondrites also reflect the incorporation of variable amounts of nucleosynthetic material (Andreasen & Sharma, 2006; Carlson *et al.*, 2007). An outstanding question is thus whether the non-chondritic  $^{142}\text{Nd}$  composition of terrestrial samples is representative of the bulk Earth composition or only of 'accessible' terrestrial reservoirs (i.e. the uppermost mantle and crust). In the latter scenario, a reservoir 'hidden' in the lower mantle with sub-chondritic  $\epsilon^{142}\text{Nd}$  composition would be needed to balance the super-chondritic signature of all accessible silicate reservoirs. In contrast, a non-chondritic  $^{142}\text{Nd}/^{144}\text{Nd}$  signature for the bulk Earth would obviate the need for a hidden reservoir but would contradict the long-held view that the terrestrial planets have perfectly chondritic abundances of refractory lithophile elements.

#### *The hidden reservoir model*

The hidden reservoir model was first proposed by Boyet & Carlson (2005). In this model, the authors postulate that the bulk Earth has a perfectly chondritic Sm/Nd and  $^{142}\text{Nd}/^{144}\text{Nd}$  composition. The more radiogenic  $^{142}\text{Nd}/^{144}\text{Nd}$  signature of the

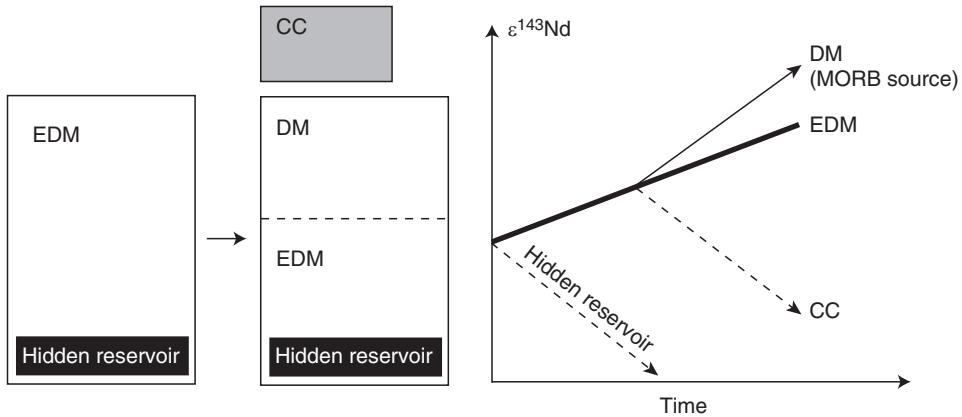


Fig. 1.18 Schematic illustration of the hidden reservoir model and the corresponding  $\epsilon^{143}\text{Nd}$  evolution of the mantle-crust system. The first stage of differentiation corresponds to the formation of the hidden reservoir and the EDM. This generates heterogeneities in  $^{142,143}\text{Nd}$ , with the EDM evolving towards  $\epsilon^{143}\text{Nd}$  signatures more radiogenic than the chondritic primitive mantle. A second stage of mantle depletion occurs when the continental crust is extracted from the EDM. This further depletes the EDM in incompatible elements, creating a more depleted mantle reservoir (DM = MORB source). As a consequence, the  $\epsilon^{143}\text{Nd}$  composition of the EDM is necessarily lower than that of the upper mantle.

Earth's 'accessible' mantle and crust must then be balanced by an enriched complementary reservoir with sub-chondritic  $\text{Sm}/\text{Nd}$  and  $^{142}\text{Nd}/^{144}\text{Nd}$  ratios (Figure 1.18). In order to satisfy  $^{146}\text{Sm}$ - $^{142}\text{Nd}$  systematics, this hidden reservoir must have formed early ( $>4.5\text{Gyr}$ ) and remained perfectly isolated from mantle convection since its formation. The most plausible location for storing such a large reservoir is the  $D''$  layer (Tolstikhin *et al.*, 2006) and it was therefore suggested that this hypothetical reservoir could represent a recycled crustal component (Boyet & Carlson, 2005, 2006) or a basal magma ocean (Labrosse *et al.*, 2007), which remained stored at the core-mantle boundary (CMB) owing to a large density contrast with the surrounding mantle. This hypothesis is supported by the presence of positive  $^{142}\text{Nd}$  anomaly in early Archean rocks (see previous section), demonstrating the early formation and recycling of a Hadean protocrust (Caro *et al.*, 2003, 2006; Boyet & Carlson, 2005). It was also shown that a dense basaltic crust recycled in the deep mantle would be gravitationally stable, although it is doubtful that such a reservoir would remain

unsampled by mantle convection (Davaille *et al.*, 2002; Bourdon & Caro, 2007).

A major obstacle to the hidden reservoir model lies in the difficulty of establishing a plausible chronology for the formation of this reservoir (Bourdon *et al.*, 2008). This chronology must satisfy coupled  $^{146,147}\text{Sm}$ - $^{142,143}\text{Nd}$  systematics but should also be consistent with the constraints derived from  $^{182}\text{Hf}$ - $^{182}\text{W}$  on the timescale of terrestrial accretion and core formation (see the section on 'Hf-W chronology of the accretion and early differentiation of the Earth and Moon'). It is evident that the isolation of a long-lived silicate reservoir at the CMB requires that core formation was complete, which essentially precludes its formation prior to 30 to 35 Myr. It is also unlikely that an early crust could survive the giant impact, and this would delay the formation of long-lived crustal reservoirs on the Earth by  $>50\text{Myr}$  after formation of the solar system (Touboul *et al.*, 2007). An additional constraint is that the EDM should have lower  $\text{Sm}/\text{Nd}$  and  $^{143}\text{Nd}/^{144}\text{Nd}$  ratios than the modern depleted mantle ( $\epsilon^{143}\text{Nd} = +9$   $\epsilon$ -units (Salters & Stracke, 2004)), as the latter was



further depleted by continental growth (Figure 1.18b). In theory,  $^{142}\text{Nd}$  anomalies can be generated until  $\sim 4.2$  Gyr. However, late formation of the hidden reservoir would require a large degree of Sm/Nd fractionation, which in turn would generate  $\epsilon^{143}\text{Nd}$  value in the mantle higher than observed in the modern MORB source (Boyet & Carlson, 2005). This constraint puts stringent limits on the minimum age of a hidden reservoir.

A major difficulty in establishing an accurate chronology for the hidden reservoir is to estimate a realistic  $\epsilon^{143}\text{Nd}$  composition for the EDM. Boyet & Carlson (2005, 2006) estimated a model age of  $4.53 \pm 0.03$  Myr by conservatively assuming that the EDM composition is identical or lower than that of the MORB source. However, Bourdon *et al.* (2008) pointed out that the effect of continental extraction cannot be neglected, as it would further increase the  $\epsilon^{143}\text{Nd}$  composition of the upper mantle. A more realistic age determination for the hidden reservoir can be obtained in the context of the 4-reservoirs model illustrated in Figure 1.18. The composition of the EDM can be obtained from the following mass balance relationship:

$$\left(\frac{^{143}\text{Nd}}{^{144}\text{Nd}}\right)_{edm} = \left(\frac{^{143}\text{Nd}}{^{144}\text{Nd}}\right)_{cc} \phi_{cc} + \left(\frac{^{143}\text{Nd}}{^{144}\text{Nd}}\right)_{dm} \phi_{dm} \quad (23)$$

where:

$$\phi_{cc} = \frac{[\text{Nd}]_{cc}}{[\text{Nd}]_{edm}} \frac{M_{cc}}{(M_{cc} + M_{dm})} = 1 - \phi_{dm} \quad (24)$$

$M_{cc}$  is the mass of the present-day continental crust ( $M_{cc} = 2.27 \cdot 10^{22}$  kg), whilst  $M_{dm}$  is the mass of mantle depleted by extraction of the continental crust.  $[\text{Nd}]_{cc}$  and  $[\text{Nd}]_{edm}$  are the Nd concentration in the continental crust ( $[\text{Nd}]_{cc} = 20$  ppm; Rudnick & Fountain, 1995) and the early depleted mantle (EDM). As illustrated in Figure 1.18, the early depleted mantle represents a residual mantle after extraction of the hidden reservoir, whilst the modern depleted mantle (DM) is formed by extraction of the continental crust from the EDM. As a consequence, the DM is more depleted and has higher  $^{147}\text{Sm}/^{144}\text{Nd}$  and  $^{143}\text{Nd}/^{144}\text{Nd}$  ratios than

the EDM. The mass of the DM is unconstrained but a conservative model can be established by assuming that the continental crust was extracted from the whole mantle (i.e.  $M_{dm} \sim M_{edm} \sim M_{bse}$ ), which minimizes its impact on the mantle  $\epsilon^{143}\text{Nd}$  composition. The Nd concentration in the EDM is also unknown but its value is necessarily lower than that of the primitive mantle (i.e.  $[\text{Nd}]_{edm} < 1.25$  ppm). Using these very conservative parameters, the maximum  $^{143}\text{Nd}/^{144}\text{Nd}$  composition of the early depleted mantle is estimated to be  $< 0.5130$  (i.e.  $\epsilon^{143}\text{Nd} < 7$   $\epsilon$ -units) for  $[\text{Nd}]_{edm} < 1.25$  ppm and decreases to  $< 6.5$   $\epsilon$ -units for a more realistic Nd concentration in the EDM of 1 ppm (Figure 1.19). The minimum age for the hidden reservoir can then be estimated to  $4.57 \pm 0.03$  Gyr using coupled  $^{142,143}\text{Nd}$  chronometry (Figure 1.20). Thus, if we assume that the isotopic shift between terrestrial and meteoritic samples result from radioactive decay, then the Sm/Nd fractionation responsible for this isotopic effect must have taken place within a few million years after formation of the solar system. A corollary is that the hypothetical 'missing' reservoir with subchondritic Sm/Nd and  $^{142}\text{Nd}/^{144}\text{Nd}$  ratios would need to be older than the core, making it unlikely to result from an internal differentiation process such as magma ocean crystallization and/or crustal formation.

The  $^{142}\text{Nd}$  results obtained from meteorites thus open a new perspective, namely that the REE (and by extension, the refractory elements) experienced minor but significant fractionation in the accretion disk, which resulted in the observed non-chondritic  $^{142}\text{Nd}$  composition for the bulk Earth. Of course, this would not preclude the preservation of Hadean crust in the deep mantle or in ancient continental roots, but would relax the constraints on the age and size of such residual reservoir, making it easier to account for the homogeneous composition of the modern mantle. Thus, whilst  $^{146}\text{Sm}$ - $^{142}\text{Nd}$  systematics has been classically interpreted in terms of internal differentiation processes, the possibility that the terrestrial planets accreted from material that was not perfectly chondritic for Sm/Nd must also be considered.

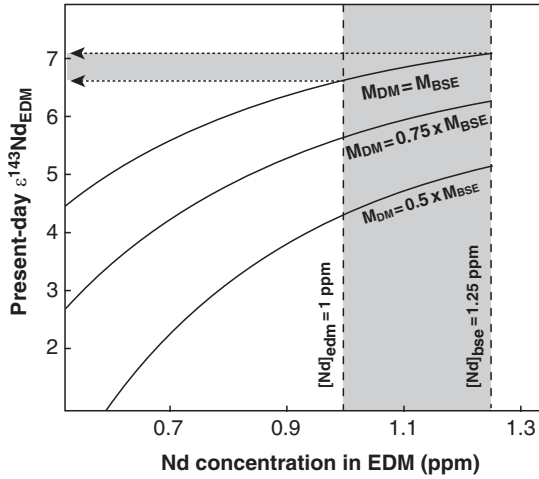


Fig. 1.19 Nd isotope mass balance showing possible  $\epsilon^{143}\text{Nd}$  compositions for the early depleted mantle (EDM) complementary to the hidden reservoir. This estimate depends on: i) the Nd concentration in the EDM after extraction of the hidden reservoir; and ii) the mass fraction of depleted mantle (i.e. MORB source) complementary to the continental crust. Both parameters are unconstrained but a maximum value for  $\epsilon^{143}\text{Nd}_{\text{EDM}}$  can be obtained assuming that the continental crust was extracted from the whole mantle (i.e.  $M_{\text{dm}} = M_{\text{bse}}$ ) and that the Nd concentration in the EDM is lower than that of the primitive mantle ( $[\text{Nd}]_{\text{edm}} < 1.25 \text{ ppm}$ ). Using these conservative parameters, a maximum  $\epsilon^{143}\text{Nd}_{\text{edm}}$  of +7 is obtained.

### *The non-chondritic Earth model*

The non-chondritic Earth hypothesis had initially been discarded based on the generally accepted view that refractory lithophile elements are present in perfectly chondritic abundances in the terrestrial planets. Whilst this is probably a correct approximation within  $\pm 10\%$ , the homogeneity of bulk chondrites should not obscure the fact that the REE did experience substantial fractionation in the solar nebula. The constitutive components of chondrites (chondrules, CAIs) show fractionated REE pattern (Figure 1.21) (Ireland *et al.*, 1988; Krestina *et al.*, 1997, 1999; Amelin & Rotenberg, 2004), indicating that the material incorporated in chondrite parent bodies

was not perfectly homogeneous for Sm/Nd. This also demonstrates that the refractory nature of the REE is by no means evidence that these elements did not fractionate in the solar nebula. It should also be noted that the terrestrial planets did not accrete from chondritic material but from differentiated planetesimals (Chambers, 2001). Thus, very early fractionation of refractory lithophile elements could have been produced during the first million years by preferential loss of the planetesimal's crusts during impacts (O'Neill & Palme, 2008) or, alternatively, by explosive volcanism (Warren, 2008), and would thus not necessarily involve volatility-controlled processes.

The magnitude of Sm/Nd fractionation needed to produce an  $18 \pm 5 \text{ ppm}$   $^{142}\text{Nd}$  excess can be estimated from Equation (11). This yields a  $^{147}\text{Sm}/^{144}\text{Nd}$  value of  $0.209 \pm 3$ , which corresponds to a 4 to 7% fractionation compared with the chondritic value. In contrast, the total range of  $^{147}\text{Sm}/^{144}\text{Nd}$  measured in bulk chondrites is  $\sim 4\%$  with most values ranging between 0.19 and 0.20 (Jacobsen & Wasserburg, 1984; Patchett *et al.*, 2004; Boyet & Carlson, 2005; Carlson *et al.*, 2007). The Sm/Nd composition required to generate an 18 ppm excess in all terrestrial samples is therefore slightly higher than the average chondritic composition but remain well within the fractionation range observed in chondrite components (Figure 1.21).

A critical test for the non-chondritic Earth model comes from the examination of  $^{142}\text{Nd}$  systematics in lunar and Martian samples. It was indeed expected that if the Earth inherited a non-chondritic Sm/Nd composition during its accretion, then the Moon (and possibly Mars) may also be characterized by superchondritic Sm/Nd and  $^{142}\text{Nd}/^{144}\text{Nd}$  ratios. If, on the other hand, these planets formed from chondritic material, then planetary isochrons for Mars and the Moon should have a common intercept corresponding to the chondritic value (i.e.  $\epsilon^{142}\text{Nd} = -18 \text{ ppm}$ ,  $^{147}\text{Sm}/^{144}\text{Nd} = 0.1966$ ). As illustrated in Figures 1.22a and b, lunar and Martian samples define correlations in an  $\epsilon^{142}\text{Nd}$  vs Sm/Nd diagram. If interpreted as an isochron relationship, the array defined by

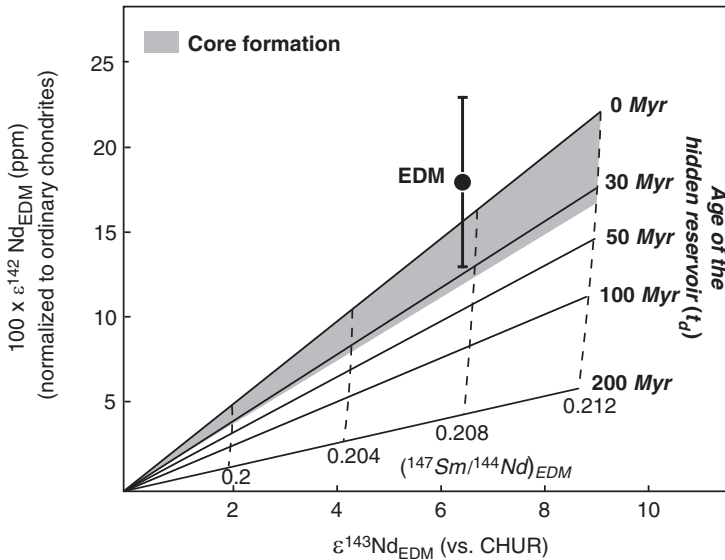


Fig. 1.20 Estimation of the age of the hidden reservoir using coupled  $^{146,147}\text{Sm}$ - $^{142,143}\text{Nd}$  systematics. The EDM is constrained to have an  $\epsilon^{142}\text{Nd}$  excess of  $18 \pm 5$  ppm compared with ordinary chondrites. The  $^{143}\text{Nd}$  composition of the EDM is necessarily lower than  $+7$   $\epsilon$ -units (Figure 1.19). This constrains the youngest possible age for the hidden reservoir to  $4.57 \pm 0.03$  Gyr.

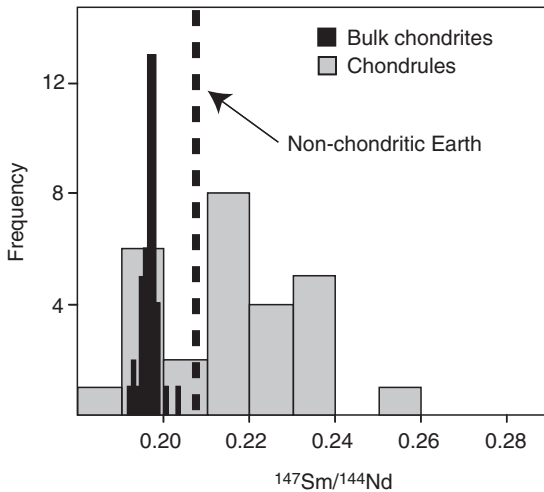
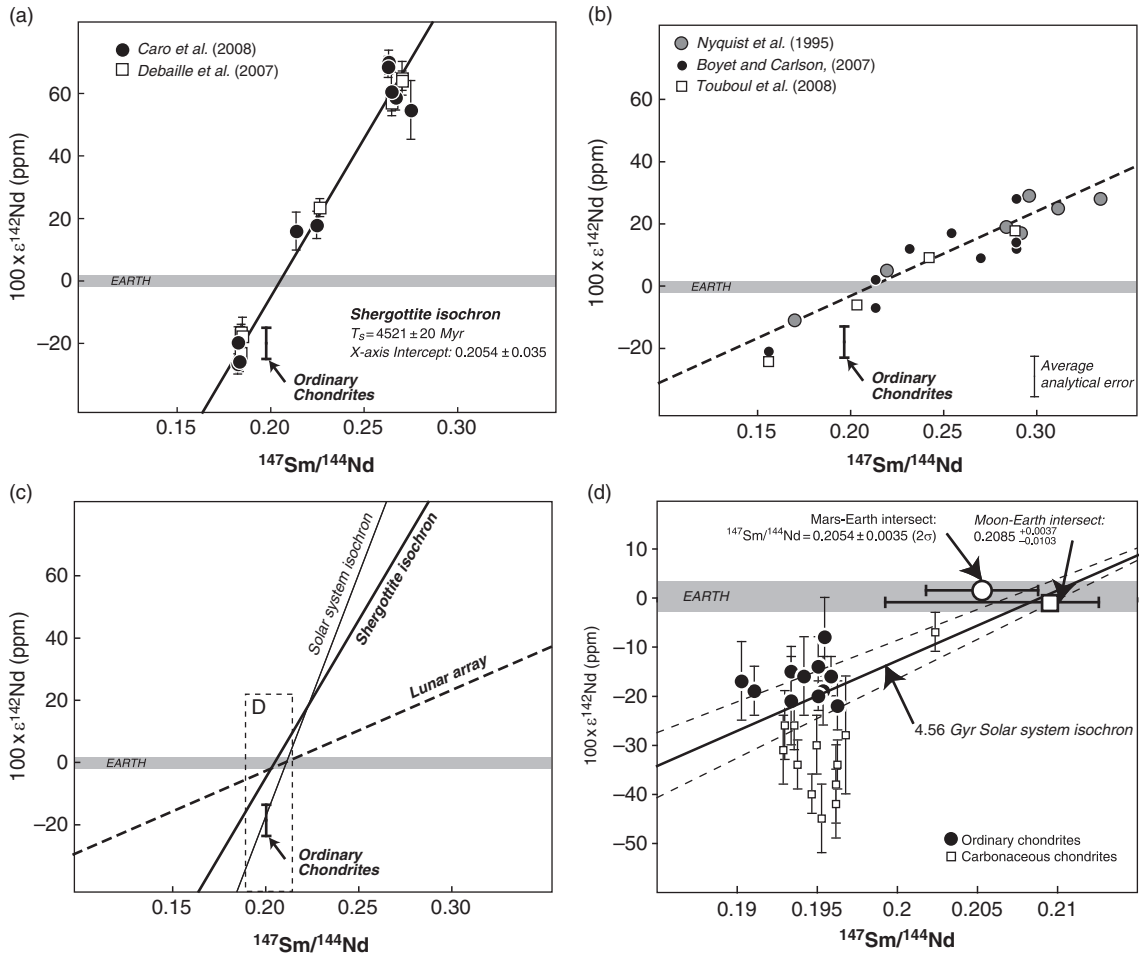


Fig. 1.21 Histogram showing the distribution of Sm/Nd ratios in bulk chondrites and chondrules. Note that chondrule composition is systematically biased towards higher Sm/Nd values. A hypothetical bulk Earth composition consistent with the observed  $^{142}\text{Nd}$  excess of  $+18$  ppm is shown for comparison. (Jacobsen & Wasserburg, 1984; Krestina *et al.*, 1997, 1999; Amelin & Rotenberg, 2004; Patchett *et al.*, 2004; Carlson *et al.*, 2007).

Shergottites yields an age of differentiation for the Martian mantle of  $4.52 \pm 0.02$  Gyr (Figure 1.22a) (Foley *et al.*, 2005a; Debaille *et al.*, 2007; Caro *et al.*, 2008). This is consistent with the presence of small  $\epsilon^{182}\text{W}$  anomalies in Martian meteorites, as these can only be produced prior to 4.5 Gyr. The  $^{142}\text{Nd}$  systematics of lunar samples and their chronological significance is more ambiguous and is currently a matter of debate. The first attempt to study the  $^{142}\text{Nd}$  composition of lunar basalts showed a well-defined correlation which, if interpreted as an isochron, would yield an age of differentiation of  $4.33 \pm 0.04$  Gyr for the lunar magma ocean (Nyquist *et al.*, 1995; Rankenburg *et al.*, 2006; Boyet & Carlson, 2007) (Figure 1.22b). This general trend has been confirmed using higher precision mass spectrometric techniques (Rankenburg *et al.*, 2006; Boyet & Carlson, 2007; Touboul *et al.*, 2009a). However, the chronological significance of this array has been put into question (Boyet & Carlson, 2007), as the estimated age of differentiation postdates the formation of the oldest lunar anorthosites by  $>100$  Myr (Carlson & Lugmair, 1988). A possible interpretation is that the primordial isochron



**Fig. 1.22**  $^{146,147}\text{Sm}$ - $^{142,143}\text{Nd}$  arrays for Mars and the Moon compared with terrestrial and chondritic compositions. (a) The isochron relationship defined by Shergottites yields an age of differentiation of  $4.52 \pm 0.02$  Gyr, reflecting crystallization of the Martian magma ocean near the end of accretion. This isochron passes above the chondritic reference value, suggesting that the Martian reservoirs sampled by Shergottites differentiated from a slightly super-chondritic mantle. (b) Lunar array defined by mare basalts (Hi-Ti and Low-Ti) and KREEP basalts. Data with large neutron corrections ( $>10$  ppm) are excluded from the regression. (c) Planetary isochrons obtained from lunar, Martian and terrestrial samples converge towards a common value corresponding to  $\epsilon^{142}\text{Nd} \approx 0$  and  $^{147}\text{Sm}/^{144}\text{Nd} \approx 0.21$ . (d) The intersects between the lunar and Martian arrays and the terrestrial composition plot within errors on a solar system isochron passing through the O-chondrite composition. This suggests that Mars and the Earth-Moon system developed a slightly fractionated Sm/Nd composition at a very early stage of planetary accretion.

relationship was partially reset by remelting and mixing of magma ocean cumulates, resulting from gravitational instabilities (Bourdon *et al.*, 2008). Regardless of the chronological signifi-

cance of the lunar array, it is evident that most lunar samples have a superchondritic  $^{142}\text{Nd}$  composition, roughly centered on the terrestrial value. This is a crucial observation showing that

the super-chondritic  $^{142}\text{Nd}$  signature observed in all terrestrial samples is probably not restricted to the uppermost mantle and crust, but more likely represents the isotopic signature of the entire Earth-Moon system.

As illustrated in Figure 1.22c, a more detailed examination of planetary data reveals that lunar and Martian isochrons intersect at an  $\epsilon^{142}\text{Nd}$  composition of +20ppm compared with ordinary chondrites, and thus define a triple intersect with the terrestrial composition. In detail, the intersect between the Martian isochron and the terrestrial value corresponds to a slightly super-chondritic  $^{147}\text{Sm}/^{144}\text{Nd}$  ratio of  $0.2054 \pm 0.0035$ , whilst the intersect defined by the lunar isochron corresponds to a similar but less precise value of 0.2085 (Figure 1.22d). Both plot within error on a 4.56 Gyr solar system isochron passing through the chondritic composition, which is precisely what would be expected if all three planets had accreted from material with super-chondritic Sm/Nd ratio. Of course, these compositions remain hypothetical as Mars and the Moon may not necessarily have perfectly 'terrestrial'  $^{142}\text{Nd}/^{144}\text{Nd}$  signatures (Bourdon *et al.*, 2008). Despite this uncertainty, the seemingly super-chondritic  $^{142}\text{Nd}$  compositions of Mars, the Earth and the Moon challenge the conventional view that terrestrial planets have rigorously chondritic abundances of refractory lithophile elements. Future research will thus need to investigate possible mechanisms for refractory elements fractionation during planetary accretion and their consequences in terms of planetary composition. A revision of the Sm-Nd parameters for the bulk Earth would, for example, require a revision of the Lu/Hf, Rb/Sr and possibly Th/U ratios of the bulk silicate Earth, which would modify our perspective on the isotopic systematics in mantle derived rocks. As illustrated in Figure 1.12b, a bulk silicate Earth with Sm/Nd ratio ~6% higher than chondritic would provide a good match to the  $^{143}\text{Nd}$  evolution of the mantle prior to 2.5 Gyr, suggesting that the Archean mantle was less depleted than previously thought. The presence of a large continental volume prior to 3 Gyr would thus no longer be required to explain the  $^{143}\text{Nd}$  signal in

Archean rocks, thereby resolving the long-held paradox of the seemingly depleted signature of the Archean mantle, despite the lack of a large stable continental mass of that age.

## CONCLUSIONS

The Earth's mantle exhibits an elevated Hf/W ratio and a small but well resolvable  $^{182}\text{W}$  excess relative to chondrites, demonstrating that at least parts of the Earth's core segregated during the lifetime of  $^{182}\text{Hf}$ . The  $^{182}\text{W}$  excess of the Earth's mantle is about one order of magnitude smaller than excesses found in the silicate part of some of the oldest planetary objects (the parent bodies of differentiated meteorites). This observation is difficult to explain unless formation of the Earth's core was protracted and involved some re-equilibration of newly accreted metal cores within the terrestrial magma ocean. The two-stage model age of the Earth's core of ~30 Myr assumes that the core formed in a single instant at the end of accretion and as such is not appropriate for modeling the continuous segregation of the Earth's core during protracted accretion. The two-stage model age, nevertheless, is useful because it provides the earliest time at which core formation can have been complete.

Determining the rate of the Earth's accretion and timing of core formation based on the  $^{182}\text{W}$  excess of the Earth's mantle requires knowledge of a number of parameters, including the degree to which the metal cores of newly accreted bodies equilibrated with the Earth's mantle and the timescales and conditions of core formation of the material that accreted to form the Earth. Our incomplete understanding of these processes makes determining an Hf-W age of the Earth's core uncertain. Additional constraints on the rate of the Earth's accretion are required and are provided by the age of the Moon. The indistinguishable W isotopic compositions of the bulk silicate Moon and Earth in conjunction with their different Hf/W ratios require that the Moon formed late, >50 Myr after solar system formation. The late age of the Moon reveals that the Hf-W

systematics of the Earth's mantle can be accounted for in two types of models. Either the Earth's accretion took place by collisions that occurred at a slowly decreasing exponential rate with a mean-life of ~40 Myr, or an initial rapid growth was followed by a long hiatus before the final, late Moon-forming impact. A better understanding of the physics and chemistry involved in metal segregation during large impacts may help distinguishing between these two scenarios.

Ubiquitous  $^{142}\text{Nd}$  anomalies in early Archean rocks from West Greenland witness an episode of mantle-crust differentiation 30 to 100 Myr after formation of the solar system. This age constraint is identical within errors to the age of differentiation of the Martian mantle, suggesting that both planets experienced early differentiation following magma ocean crystallization. The preservation of positive  $^{142}\text{Nd}$  anomalies in the mantle until 3.6 Gyr requires that the Hadean crust was a long-lived reservoir with a lifetime of ~1 Gyr. The lack of  $^{142}\text{Nd}$  heterogeneities in the late Archean mantle, if confirmed, would suggest that this early crust was compositionally more mafic than modern continents and was extensively recycled prior to the major episode of crustal growth 2.5 to 3 Gyr ago.

The radiogenic excess of ~20 ppm measured in all 'accessible' terrestrial reservoirs suggests that part or all of the Earth's mantle evolved with an Sm/Nd ratio 4 to 7% higher than chondritic for at least 4.53 Gyr. This early fractionation thus occurred before the Earth's core had completely segregated and also prior to the giant Moon-forming impact. This is difficult to explain unless the non-chondritic Sm/Nd composition of the Earth was inherited from accreting material (most likely the planetary embryos) rather than generated at a later stage by internal differentiation. As a consequence, the assumption of a chondritic Hf/W ratio of the bulk Earth may not be valid. A non-chondritic Earth would have a Hf/W ratio ~1.5 times higher than chondritic and also the Hf/W ratio of the bulk silicate Earth, which is estimated assuming a chondritic ratios of refractory lithophile elements, would be ~1.5 times higher (Kleine *et al.*, 2009). For a non-chondritic Earth, Hf-W ages become younger compared to a

chondritic Earth (e.g. the two-stage model age is ~40 Myr instead of ~30 Myr) but given the uncertainties inherent in Hf-W models for the Earth's accretion and core formation, this does not affect the main conclusions drawn here.

Martian and lunar samples define linear arrays in an  $\epsilon^{142}\text{Nd}$  vs Sm/Nd plot, which can be interpreted as planetary isochrons dating the crystallization of magma oceans on these planets. The Martian array yields an age of differentiation of 4.52 Gyr, in agreement with the presence of  $^{182}\text{W}$  anomalies in these samples. The lunar array, on the other hand, yields a surprisingly young age of 4.35 Gyr. The chronological significance of this trend is uncertain as it could represent a mixing relationship between magma ocean cumulates rather than a true isochron. An important observation, however, is that the Martian and lunar arrays do not intersect the chondritic reference composition, as would be expected if both planets had chondritic Sm/Nd and  $^{142}\text{Nd}/^{144}\text{Nd}$  ratios. These arrays define a common intersect with the terrestrial value (at  $\epsilon^{142}\text{Nd} = 0$  and  $^{147}\text{Sm}/^{144}\text{Nd} = 0.208$ ), defining a plausible bulk composition for Mars and the Earth-Moon system. This observation supports the view that refractory lithophile elements in all the terrestrial planets may have experienced minor fractionation during accretion, which ultimately resulted in the super-chondritic  $^{142}\text{Nd}/^{144}\text{Nd}$  signature of the Earth's mantle.

#### ACKNOWLEDGMENTS

Discussions with B. Bourdon, M. Touboul, B. Marty and many other colleagues are gratefully acknowledged. The paper benefited from constructive reviews by V. Bennett and an anonymous reviewer. Informal review of the manuscript by J. Marin was greatly appreciated.

#### REFERENCES

- Abe Y. 1997. Thermal and chemical evolution of the terrestrial magma ocean. *Physics of the Earth and Planetary Interiors* **100**: 27–39.

- Agnor CB, Canup RM, Levison, HF. 1999. On the character and consequences of large impacts in the late stage of terrestrial planet formation. *Icarus* **142**: 219–237.
- Albarede F. 1995. *Introduction to Geochemical Modeling*. Cambridge University Press, Cambridge.
- Albarede F. 2001. Radiogenic ingrowth in systems with multiple reservoirs: applications to the differentiation of the crust-mantle system. *Earth and Planetary Science Letters* **189**: 59–73.
- Albarede F, Rouxel, M. 1987. The Sm/Nd secular evolution of the continental crust and the depleted mantle. *Earth and Planetary Science Letters* **82**: 25–35.
- Allegre CJ, Othman DB, Polve M, Richard D. 1979. Nd-Sr isotopic correlation in mantle materials and geodynamic consequences. *Physics of the Earth and Planetary Interiors* **19**: 293–306.
- Amelin Y, Rotenberg, E. 2004. Sm-Nd systematics of chondrites. *Earth and Planetary Science Letters* **223**: 267–282.
- Amelin Y, Krot AN, Hutcheon ID, Ulyanov AA. 2002. Lead isotopic ages of chondrules and calcium-aluminum-rich inclusions. *Science* **297**: 1679–1683.
- Andreasen R, Sharma M. 2006. Solar nebula heterogeneity in p-process samarium and neodymium isotopes. *Science* **314**: 806–809.
- Armstrong RL. 1981. The case for crustal recycling on a near-steady-state no-continental-growth Earth. *Philosophical Transactions of the Royal Society* **A301**: 443–472.
- Asplund M, Grevesse N, Sauval AJ. 2006. The solar chemical composition. *Nuclear Physics A* **777**: 1–4.
- Bennett VC. 2003. Compositional evolution of the mantle. In: *The Mantle and Core*, Carlson RW (ed.), Vol. 2, *Treatise on Geochemistry*, Holland HD, Turekian KK (eds), Elsevier-Perigamon, Oxford.
- Bennett VC, Nutman AP, McCulloch MT. 1993. Nd isotopic evidence for transient, highly depleted mantle reservoirs in the early history of the Earth. *Earth and Planetary Science Letters* **119**: 299–317.
- Bennett VC, Brandon AD, Nutman AP. 2007. Coupled  $^{142}\text{Nd}$ - $^{143}\text{Nd}$  isotopic evidence for Hadean mantle dynamics. *Science* **318**: 1907–1910.
- Birck J-L. 2004. An overview of isotopic anomalies in extraterrestrial materials and their nucleosynthetic heritage. In: *Geochemistry of Non-traditional Stable Isotopes*. Johnson, C-M, Beard BL, Albarede F. (eds), Mineralogical Society of America, Geochemical Society.
- Bourdon B, Caro G. 2007. The early terrestrial crust. *C. R. Geosciences* **339**: 928–936.
- Bourdon B, Touboul M, Caro G, Kleine T. 2008. Early differentiation of the Earth and the Moon. *Philosophical Transactions of the Royal Society* **366**: 4105–4128.
- Bouvier A, Blichert-Toft J, Moynier F, Vervoort JD, Albarède F. 2007. Pb-Pb dating constraints on the accretion and cooling history of chondrites. *Geochimica et Cosmochimica Acta* **71**: 1583–1604.
- Bowring SA, Housh T. 1995. The Earth's early evolution. *Science* **269**: 1535–1540.
- Boyet M, Blichert-Toft J, Rosing M, Storey CD, Télouk M, Albarede F. 2004.  $^{142}\text{Nd}$  evidence for early Earth differentiation. *Earth and Planetary Science Letters* **214**: 427–442.
- Boyet M, Carlson RW. 2006. A new geochemical model for the Earth's mantle inferred from  $^{146}\text{Sm}$ - $^{142}\text{Nd}$  systematics. *Earth and Planetary Science Letters* **250**: 254–268.
- Boyet M, Carlson RW. 2007. A highly depleted moon or a non-magma ocean origin for the lunar crust? *Earth and Planetary Science Letters* **262**: 505–516.
- Boyet M, Carlson RW. 2005.  $^{142}\text{Nd}$  evidence for early (>4.53 Ga) global differentiation of the silicate Earth. *Science* **214**: 427–442.
- Boynton WV. 1975. Fractionation in the solar nebula: Condensation of yttrium and the rare earth elements. *Geochimica et Cosmochimica Acta* **39**: 569–584.
- Brandon AD, Humayun M, Puchtel IS, Leya I, Zolensky M. 2005. Osmium isotope evidence for an s-process carrier in primitive chondrites. *Nature* **309**: 1233–1236.
- Burkhardt C, Kleine T, Palme H, et al. 2008. Hf-W mineral isochron for Ca,Al-rich inclusions: Age of the solar system and the timing of core formation in planetesimals. *Geochimica et Cosmochimica Acta* **72**: 6177–6197.
- Canup RM. 2004. Dynamics of lunar formation. *Annual Review of Astronomy and Astrophysics* **42**: 441–475.
- Canup RM, Asphaug E. 2001. Origin of the Moon in a giant impact near the end of the Earth's formation. *Nature* **412**: 708–712.
- Carlson RW, Lugmair GW. 1988. The age of ferroan anorthosite 60025: oldest crust on a young Moon? *Earth and Planetary Science Letters* **90**: 119–130.
- Carlson RW, Boyet M, Horan M. 2007. Chondrite barium, neodymium and samarium isotopic heterogeneity and early earth differentiation. *Science* **316**: 1175–1178.
- Caro G, Bourdon B, Birck J-L, Moorbath S. 2003.  $^{146}\text{Sm}$ - $^{142}\text{Nd}$  evidence for early differentiation of the Earth's mantle. *Nature* **423**: 428–432.

- Caro G, Bourdon B, Wood BJ, Corgne A. 2005. Trace element fractionation generated by melt segregation from a magma ocean. *Nature* **436**: 246–249.
- Caro G, Bourdon B, Birck.-L, Moorbath S. 2006. High-precision  $^{142}\text{Nd}/^{144}\text{Nd}$  measurements in terrestrial rocks: Constraints on the early differentiation of the Earth's mantle. *Geochimica et Cosmochimica Acta* **70**: 164–191.
- Caro G, Bourdon B, Halliday AN, Quitté G. 2008. Superchondritic Sm/Nd ratios in Mars, the Earth and the Moon. *Nature* **452**: 336–339.
- Chambers JE. 2001. Making more terrestrial planets. *Icarus* **152**: 205–224.
- Chambers JE. 2004. Planetary accretion in the inner solar system. *Earth and Planetary Science Letters* **223**: 241–252.
- Chase CG, Patchett PJ. 1988. Stored mafic/ultramafic crust and early Archean mantle depletion. *Earth and Planetary Science Letters* **91**: 66–72.
- Christensen UR, Hofmann AW. 1994. Segregation of subducted oceanic crust in the convecting mantle. *Journal of Geophysical Research* **99**: 19,867–19,884.
- Condie KC. 2000. Episodic growth models: after thoughts and extensions. *Tectonophysics* **322**: 153–162.
- Cottrell E, Walter M.J, Walker D. 2009. Metal-silicate partitioning of tungsten at high pressure and temperature: Implications for equilibrium core formation in Earth. *Earth and Planetary Science Letters* **281**: 275–287.
- Dauphas N, Marty B, Reisberg L. 2002. Inference on terrestrial genesis from molybdenum isotope systematics. *Geophysical Research Letters* **29**: 1084.
- Davaille A, Girard F, Le Bars M. 2002. How to anchor hotspots in a convective mantle? *Earth and Planetary Science Letters* **203**: 621–634.
- Davis AM, Grossman L. 1979. Condensation and fractionation of rare earths in the solar nebula. *Geochimica et Cosmochimica Acta* **43**: 1611–1632.
- Debaille V, Brandon AD, Yin QZ, Jacobsen, B. 2007. Coupled  $^{142}\text{Nd}$ - $^{143}\text{Nd}$  evidence for a protracted magma ocean in Mars. *Nature* **450**: 525–528.
- DePaolo DJ. 1980. Crustal growth and mantle evolution: inferences from models of element transport and Sr and Nd isotopes. *Geochimica et Cosmochimica Acta* **44**: 1185–1196.
- DePaolo DJ, Wasserburg GJ. 1979. Petrogenetic mixing models and Nd-Sr isotopic patterns. *Geochimica et Cosmochimica Acta* **43**: 615–627.
- Foley CN, Wadhwa M, Borg LE, Janney PE, Hines R, Grove TL. 2005a. The early differentiation history of Mars from W-182 Nd-142 isotope systematics in the SNC meteorites. *Geochimica et Cosmochimica Acta* **69**: 4557–4571.
- Foley CN, Wadhwa M, Borg LE, Janney PE, Hines R, Grove TL. 2005b. The early differentiation history of Mars from  $^{182}\text{W}$ - $^{142}\text{Nd}$  isotope systematics in the SNC meteorites. *Geochimica et Cosmochimica Acta* **69**: 4557–4571.
- Galer SJG, Goldstein SL. 1991. Early mantle differentiation and its thermal consequences. *Geochimica et Cosmochimica Acta* **55**: 227–239.
- Goldstein SL, Galer SJG. 1992. On the trail of early mantle differentiation:  $^{142}\text{Nd}/^{144}\text{Nd}$  ratios of early Archean rocks. *Eos Transactions AGU* **73**: S323.
- Halliday AN. 2004. Mixing, volatile loss and compositional change during impact-driven accretion of the Earth. *Nature* **427**: 505–509.
- Halliday AN. 2008. A young Moon-forming giant impact at 70–110 million years accompanied by late-stage mixing, core formation and degassing of the Earth. *Philosophical Transactions of the Royal Society* **366**: 4205–4252.
- Halliday A, Rehkämper M, Lee DC, Yi W. 1996. Early evolution of the Earth and Moon: New constraints from Hf-W isotope geochemistry. *Earth and Planetary Science Letters* **142**: 75–89.
- Harper CL, Jacobsen SB. 1992. Evidence from coupled  $^{147}\text{Sm}$ - $^{143}\text{Nd}$  and  $^{146}\text{Sm}$ - $^{142}\text{Nd}$  systematics for very early (4.5 Gyr) differentiation of the Earth's mantle. *Nature* **360**: 728–732.
- Harper CL, Jacobsen SB. 1996. Evidence for  $^{182}\text{Hf}$  in the early solar system and constraints on the timescale of terrestrial accretion and core formation. *Geochimica et Cosmochimica Acta* **60**: 1131–1153.
- Hofmann AW. 1988. Chemical differentiation of the Earth: the relationship between mantle, continental crust, and oceanic crust. *Earth and Planetary Science Letters* **90**: 297–314.
- Horan MF, Smoliar MI, Walker RJ. 1998.  $^{182}\text{W}$  and  $^{187}\text{Re}$ - $^{187}\text{Os}$  systematics of iron meteorites: Chronology for melting, differentiation, and crystallization in asteroids. *Geochimica et Cosmochimica Acta* **62**: 545–554.
- Ireland TR, Fahey AJ, Zinner EK, 1988. Trace element abundances in hibonites from the Murchison carbonaceous chondrite: constraints on high-temperature processes in the solar nebula. *Geochimica et Cosmochimica Acta* **52**: 2841–2854.
- Jacobsen SB. 1988. Isotopic constraints on crustal growth and recycling. *Earth and Planetary Science Letters* **90**: 315–329.



- Jacobsen SB. 2005. The Hf-W isotopic system and the origin of the Earth and Moon. *Annual Review of Earth and Planetary Sciences* **33**: 531–570.
- Jacobsen B, Wasserburg GJ. 1979. The mean age of mantle and crustal reservoirs. *Journal of Geophysical Research* **84**: 7411–7424.
- Jacobsen SB, Wasserburg GJ. 1984. Sm-Nd evolution of chondrites and achondrites, II. *Earth and Planetary Science Letters* **67**: 137–150.
- Kleine T, Münker C, Mezger K, Palme H. 2002. Rapid accretion and early core formation on asteroids and the terrestrial planets from Hf-W chronometry. *Nature* **418**: 952–955.
- Kleine T, Mezger K, Munker C, Palme H, Bischoff A. 2004a.  $^{182}\text{Hf}$ - $^{182}\text{W}$  isotope systematics of chondrites, eucrites, and Martian meteorites: Chronology of core formation and early differentiation in Vesta and Mars. *Geochimica et Cosmochimica Acta* **68**: 2935–2946.
- Kleine T, Mezger, K, Palme H, Scherer E, Münker C. 2004b. The W isotope evolution of the bulk silicate Earth: constraints on the timing and mechanisms of core formation and accretion. *Earth and Planetary Science Letters* **228**: 109–123.
- Kleine T, Mezger K, Palme H, Scherer E, Münker C. 2005a. Early core formation in asteroids and late accretion of chondrite parent bodies: Evidence from  $^{182}\text{Hf}$ - $^{182}\text{W}$  in CAIs, metal-rich chondrites and iron meteorites. *Geochimica et Cosmochimica Acta* **69**: 5805–5818.
- Kleine T, Palme H, Mezger K, Halliday AN. 2005b. Hf-W chronometry of lunar metals and the age and early differentiation of the Moon. *Science* **310**: 1671–1674.
- Kleine T, Touboul M, Bourdon B, *et al.* 2009. Hf-W chronology of the accretion and early evolution of asteroids and terrestrial planets. *Geochimica et Cosmochimica Acta* **73**: 5150–5188.
- Krestina N, Jagoutz E, Kurat G. 1997. Sm-Nd system in chondrules from Bjurböle L4 chondrite. *Proceedings of Lunar and Planetary Science XXVIII*, 1659.
- Krestina N, Jagoutz E, Kurat G. 1999. The interrelation between core and rim of individual chondrules from the different meteorites in term of Sm-Nd isotopic system. *Proceedings of Lunar and Planetary Science XXX*, 1918.
- Labrosse S, Herlund JW, Coltice N. 2007. A crystallizing dense magma ocean at the base of the Earth's mantle. *Nature* **450**: 866–869.
- Lee DC, Halliday AN. 1995. Hafnium-tungsten chronometry and the timing of terrestrial core formation. *Nature* **378**: 771–774.
- Lee DC, Halliday AN. 1997. Core formation on Mars and differentiated asteroids. *Nature* **388**: 854–857.
- Lee DC, Halliday AN, Snyder GA, Taylor LA. 1997. Age and origin of the moon. *Science* **278**: 1098–1103.
- Lodders K, Fegley B. 1993. Lanthanide and actinide chemistry at high C/O ratios in the solar nebula. *Earth and Planetary Science Letters* **117**: 125–145.
- Lugmair GW, Marti K. 1977. Sm-Nd-Pu timepieces in the Angra Dos Reis meteorite. *Earth and Planetary Science Letters* **35**: 273–284.
- Lugmair GW, Scheinin NB, Marti K. 1983. Samarium-146 in the early solar system: Evidence from Neodymium in the Allende meteorite. *Science* **222**: 1015–1018.
- Lugmair GW, Galer SJG., 1992. Age and isotopic relationships among the angrite Lewis Cliff 86010 and Angra Dos Reis. *Geochimica et Cosmochimica Acta* **56**: 1673–1694.
- Markowski A, Quitté G, Halliday AN, Kleine T. 2006. Tungsten isotopic compositions of iron meteorites: chronological constraints vs cosmogenic effects. *Earth and Planetary Science Letters* **242**: 1–15.
- Markowski A, Quitté G, Kleine T, Halliday A, Bizzarro M, Irving AJ. 2007. Hf-W chronometry of angrites and the earliest evolution of planetary bodies. *Earth and Planetary Science Letters* **262**: 214–229.
- McCulloch MT, Bennett VC. 1993. Evolution of the early Earth: constraints from  $^{143}\text{Nd}$ - $^{142}\text{Nd}$  isotopic systematics. *Lithos* **30**: 237–255.
- McDonough WF, Sun S-S. 1995. The composition of the Earth. *Chemical Geology* **120**: 223–253.
- Moorbath S, Whitehouse MJ, Kamber BS. 1997. Extreme Nd-isotope heterogeneity in the early Archaean – Fact of fiction? Case histories from northern Canada and West Greenland. *Chemical Geology* **135**: 213–231.
- Newsom HE, Sims KWW, Noll P, Jaeger W, Maehr S, Beserra T. 1996. The depletion of W in the bulk silicate Earth: constraints on core formation. *Geochimica et Cosmochimica Acta* **60**: 1155–1169.
- Nimmo F, Agnor CB. 2006. Isotopic outcomes of N-body accretion simulations: Constraints on equilibration processes during large impacts from Hf/W observations. *Earth and Planetary Science Letters* **243**: 26–43.
- Nimmo F, Kleine T. 2007. How rapidly did Mars accrete? Uncertainties in the Hf-W timing of core formation. *Icarus* **191**: 497–504.
- Norman MD, Borg LE, Nyquist LE, Bogard DD. 2003. Chronology, geochemistry, and petrology of a ferroan noritic anorthosite clast from Descartes breccia

- 67215: Clues to the age, origin, structure, and impact history of the lunar crust. *Meteoritics and Planetary Science* **38**: 645–661.
- Nyquist LE, Bansal B, Wiesmann H, Shih C-Y. 1994. Neodymium, Strontium and Chromium isotopic studies of the LEW86010 and Angra Dos Reis meteorites and the chronology of the angrite parent body. *Meteoritics* **29**: 872–885.
- Nyquist LE, Wiesmann H, Bansal B, Shih C-Y, Keith JE, Harper CL. 1995.  $^{146}\text{Sm}$ - $^{142}\text{Nd}$  formation interval for the lunar mantle. *Geochimica et Cosmochimica Acta* **13**: 2817–2837.
- O'Neil J, Carlson RW, Francis D, Stevenson RK. 2008. Neodymium-142 evidence for Hadean mafic crust. *Science* **321**: 1821–1831.
- O'Neill HSC, Palme H. 2008. Collisional erosion and the non-chondritic composition of the terrestrial planets. *Philosophical Transactions of the Royal Society* **366**: 4205–4238.
- Ozima M, Podosek FA. 1999. Formation age of the Earth from  $^{129}\text{I}/^{127}\text{I}$  and  $^{244}\text{Pu}/^{238}\text{U}$  systematics and the missing Xe. *Journal of Geophysical Research* **104**: 25,493–25,499.
- Pack A, Shelley JMG, Palme H. 2004. Chondrules with peculiar REE patterns: Implications for solar nebular condensation at high C/O. *Science* **303**: 997–1000.
- Pahlevan K, Stevenson DJ. 2007. Equilibration in the aftermath of the lunar-forming giant impact. *Earth and Planetary Science Letters* **262**: 438–449.
- Patchett PJ, Vervoort JD, Söderlund U, Salters VJM. 2004. Lu-Hf and Sm-Nd isotopic systematics in chondrites and their constraints on the Lu-Hf properties of the Earth. *Earth and Planetary Science Letters* **202**: 345–360.
- Prinzhofer DA, Papanastassiou DA, Wasserburg G.J. 1989. The presence of  $^{146}\text{Sm}$  in the early solar system and implications for its nucleosynthesis. *Astrophysics Journal* **344**: L81–L84.
- Prinzhofer DA, Papanastassiou DA, Wasserburg G.J. 1992. Samarium-Neodymium evolution of meteorites. *Geochimica et Cosmochimica Acta* **56**: 797–815.
- Ranen MC, Jacobsen SB. 2006. Barium isotopes in chondritic meteorites: implications for planetary reservoir models. *Science* **314**: 809–812.
- Rankenburg K, Brandon AD, Neal CR. 2006. Neodymium isotope evidence for a chondritic composition of the Moon. *Science* **312**: 1369–1372.
- Regelous M, Collerson KD. 1996.  $^{147}\text{Sm}$ - $^{143}\text{Nd}$ ,  $^{146}\text{Sm}$ - $^{142}\text{Nd}$  systematics of early Archean rocks and implications for crust-mantle evolution. *Geochimica et Cosmochimica Acta* **60**: 3513–3520.
- Reisberg L, Dauphas N, Luguet A, Pearson DG, Gallino R, Zimmermann C. 2009. Nucleosynthetic osmium isotope anomalies in acid leachates of the Murchison meteorite. *Earth and Planetary Science Letters* **277**: 334–344.
- Rubie DC, Gessmann CK, Frost DJ. 2004. Partitioning of oxygen during core formation on the Earth and Mars. *Nature* **429**: 58–61.
- Rubie DC, Nimmo F, Melosh HJ, Gerald S. 2007. *Formation of Earth's Core, Treatise on Geophysics*. Elsevier, Amsterdam, 51–90.
- Rudnick RL, Fountain DM. 1995. Nature and composition of the continental crust: a lower crustal perspective. *Reviews in Geophysics* **33**: 267–309.
- Salters VJM, Stracke A. 2004. Composition of the depleted mantle. *Geochemistry Geophysics Geosystems* **5**: doi: 10.1029/2003GC000597.
- Schersten A, Elliott T, Hawkesworth C, Russell S.S, Masarik J. 2006. Hf-W evidence for rapid differentiation of iron meteorite parent bodies. *Earth and Planetary Science Letters* **241**: 530–542.
- Schoenberg R, Kamber BS, Collerson KD, Eugster O. 2002. New W-isotope evidence for rapid terrestrial accretion and very early core formation. *Geochimica et Cosmochimica Acta* **66**: 3151–3160.
- Sharma M, Papanastassiou DA, Wasserburg GJ, Dymek RF. 1996. The issue of the terrestrial record of  $^{146}\text{Sm}$ . *Geochimica et Cosmochimica Acta* **60**: 2037–2047.
- Shirey SB, Hanson GN. 1986. Mantle heterogeneity and crustal recycling in Archean granite-greenstone belts in the Rainy Lake area, superior province, Ontario, Canada. *Geochimica et Cosmochimica Acta* **50**: 2631–2651.
- Solomatov VS. 2000. Fluid dynamics of a terrestrial magma ocean. In: *Origin of the Earth and Moon*, RM, Righter K (eds), The University of Arizona Press, Arizona, Tucson 323–338.
- Staudacher T, Allegre C.J. 1982. Terrestrial xenology. *Earth and Planetary Science Letters* **60**: 5391–5406.
- Stevenson DJ. 1990. Fluid dynamics of core formation. In: *Origin of the Earth*, Newsom HE, Jones JE (eds), Oxford University Press, New York, 231–249.
- Taylor SR, McLennan SM. 1985. *The Continental Crust: Its Composition And Evolution*. Blackwell Scientific Publications, Oxford.
- Tolstikhin IN, Kramers JD, Hofmann AW. 2006. A chemical Earth model with whole mantle convection: The importance of a core-mantle boundary layer (D'') and its early formation. *Chemical Geology* **226**: 79–99.

- Tonks W, Melosh HJ. 1993. Magma ocean formation due to giant impacts. *Journal of Geophysical Research* **98**: 5319–5333.
- Touboul M, Kleine T, Bourdon B, Palme H, Wieler R. 2007. Late formation and prolonged differentiation of the Moon inferred from W isotopes in lunar metals. *Nature* **450**: 1206–1209.
- Touboul M, Kleine T, Bourdon B. 2008. Hf-W systematics of cumulate eucrites and the chronology of the eucrite parent body. *Lunar and Planetary Science Conference XXXIX*.
- Touboul M, Kleine T, Bourdon B, Nyquist LE, Shih C-Y. 2009a. New  $^{142}\text{Nd}$  evidence for a non-chondritic composition of the Moon. *40th Lunar and Planetary Science Conference*, Abstract No, 2269.
- Touboul M, Kleine T, Bourdon B, Palme H, Wieler R. 2009b. Tungsten isotopes in ferroan anorthosites: Implications for the age of the Moon and lifetime of its magma ocean. *Icarus* **199**: 245–249.
- Upadhyay D, Scherer EE, Mezger K. 2009.  $^{142}\text{Nd}$  evidence for an enriched Hadean reservoir in cratonic roots. *Nature* **459**: 1118–1121.
- Wade J, Wood BJ. 2005. Core formation and the oxidation state of the Earth. *Earth and Planetary Science Letters* **236**: 78–95.
- Warren PH. 2008. A depleted, not ideally chondritic bulk Earth: The explosive-volcanic basalt loss hypothesis. *Geochimica et Cosmochimica Acta* **72**: 2217–2235.
- Wetherill GW. 1990. Formation of the Earth. *Annual Review of Earth and Planetary Sciences* **18**: 205–256.
- Wilde SA, Valley JW, Peck WH, Graham CM. 2001. Evidence from detrital zircons for the existence of continental crust and oceans on the Earth 4.4 Gyr ago. *Nature* **409**: 175–178.
- Wood BJ, Wade J, Kilburn MR. 2008. Core formation and the oxidation state of the Earth: Additional constraints from Nb, V and Cr partitioning. *Geochimica et Cosmochimica Acta* **72**: 1415–1426.
- Yin QZ, Jacobsen SB, Yamashita K. 2002a. Diverse supernova sources of pre-solar material inferred from molybdenum isotopes in meteorites. *Nature* **415**: 881–883.
- Yin QZ, Jacobsen SB, Yamashita K, Blichert-Toft J, Télouk P, Albarède F. 2002b. A short timescale for terrestrial planet formation from Hf-W chronometry of meteorites. *Nature* **418**: 949–952.
- Zindler A, Hart S. 1986. Chemical geodynamics. *Annual Reviews in Earth Planetary Science* **14**: 493–571.